AD_____

Award Number: DAMD17-98-1-8245

TITLE: Role of Autocrine Motility Factor in Osteolytic Metastasis

PRINCIPAL INVESTIGATOR: John Chirgwin, Ph.D.

CONTRACTING ORGANIZATION: The University of Texas Health Science Center at San Antonio
San Antonio, Texas 78284-7828

REPORT DATE: April 2000

TYPE OF REPORT: Annual

PREPARED FOR: U.S. Army Medical Research and Materiel Command
Fort Detrick, Maryland 21702-5012

REPORT DOCUMENTATION PAGE

Form Approved
OMB No. 074-0188

1. AGENCY USE ONLY (Leave blank)	2. REPORT DATE	3. REPORT TYPE AND DATES COVERED
	April 2000	Annual (1 Apr 99 - 31 Mar 00)

4. TITLE AND SUBTITLE
Role of Autocrine Motility Factor in Osteolytic Metastasis

5. FUNDING NUMBERS
DAMD17-98-1-8245

6. AUTHOR(S)
John Chirgwin, Ph.D.

7. PERFORMING ORGANIZATION NAME(S) AND ADDRESS(ES)
The University of Texas Health Science Center at San Antonio
San Antonio, Texas 78284-7828

E-MAIL:
chirgwin@uthscsa.edu

8. PERFORMING ORGANIZATION REPORT NUMBER

9. SPONSORING / MONITORING AGENCY NAME(S) AND ADDRESS(ES)
U.S. Army Medical Research and Materiel Command
Fort Detrick, Maryland 21702-5012

10. SPONSORING / MONITORING AGENCY REPORT NUMBER

11. SUPPLEMENTARY NOTES

12a. DISTRIBUTION / AVAILABILITY STATEMENT
Approved for public release; distribution unlimited

12b. DISTRIBUTION CODE

13. ABSTRACT ***(Maximum 200 Words)***

Autocrine motility factor (AMF) is expressed by human breast cancer cells, such as MCF7 where its expression is stimulated by heregulin. Tumor cells constitutively secreting mouse AMF caused periosteal new bone formation in two different models of metastasis-an osteoblastic response similar to what is found with about 15% of breast cancers metastatic to bone. Whenever serum AMF concentrations were significantly increased, the animals displayed tumor-associated weight loss (cachexia), a major cause of morbidity and mortality in advanced disease. The effects of AMF on bone were independent of PTHrP, which plays a central role in osteolytic bone metastases. We also have determined the clearance rate of AMF from the mouse circulation. The species-specific effects of AMF remain little understood; so we undertook to clarify the stucture:function relationships involved. We cloned, sequenced and expressed rabbit AMF, for which the x-ray crystallographic data were already partially solved. These results have been published. We also developed a recombinant protein expression system for the mouse and human factors, which we now prepare in 100mg batches. The human factor has been crystallized and the x-ray structure solved to 1.8Å.

14. SUBJECT TERMS
Breast Cancer

15. NUMBER OF PAGES
50

16. PRICE CODE

17. SECURITY CLASSIFICATION OF REPORT	18. SECURITY CLASSIFICATION OF THIS PAGE	19. SECURITY CLASSIFICATION OF ABSTRACT	20. LIMITATION OF ABSTRACT
Unclassified	Unclassified	Unclassified	Unlimited

NSN 7540-01-280-5500

Standard Form 298 (Rev. 2-89)
Prescribed by ANSI Std. Z39-18
298-102

FOREWORD

Opinions, interpretations, conclusions and recommendations are those of the author and are not necessarily endorsed by the U.S. Army.

___ Where copyrighted material is quoted, permission has been obtained to use such material.

___ Where material from documents designated for limited distribution is quoted, permission has been obtained to use the material.

___ Citations of commercial organizations and trade names in this report do not constitute an official Department of Army endorsement or approval of the products or services of these organizations.

X In conducting research using animals, the investigator(s) adhered to the "Guide for the Care and Use of Laboratory Animals," prepared by the Committee on Care and use of Laboratory Animals of the Institute of Laboratory Resources, national Research Council (NIH Publication No. 86-23, Revised 1985). JMC

X For the protection of human subjects, the investigator(s) adhered to policies of applicable Federal Law 45 CFR 46. JMC

N/A In conducting research utilizing recombinant DNA technology, the investigator(s) adhered to current guidelines promulgated by the National Institutes of Health. JMC

N/A In the conduct of research utilizing recombinant DNA, the investigator(s) adhered to the NIH Guidelines for Research Involving Recombinant DNA Molecules. JMC

N/A In the conduct of research involving hazardous organisms, the investigator(s) adhered to the CDC-NIH Guide for Biosafety in Microbiological and Biomedical Laboratories. JMC

John M. Chirgwin 4/30/02

PI - Signature Date

TABLE OF CONTENTS

INTRODUCTION

Autocrine motility factor (AMF) is expressed by a wide variety of tumor cells, including several melanoma, fibrosarcoma, and prostate cancer and human MCF7 breast cancer cells, where its expression is stimulated by heregulin. It increases invasion through extracellular matrix and cell motility by a number of tumor lines. AMF is identical to a previously characterized molecule, neuroleukin, which is secreted by stimulated lymphocytes and is in turn the extracellular form of phosphoglucose isomerase, a glycolytic enzyme. The pathway of secretion of AMF is unknown but may follow a nonclassical route, similar to that taken out of cells by FGFs 1 & 2. Serum phosphoglucose isomerase levels were used as a marker of metastatic breast disease over 40 years ago and found to correlate with the growth of tumor in bone. Since AMF is secreted by multiple tumor types by an unknown mechanism, it has not been developed as a useful prognostic marker.

Our work is the first to test a role in vivo for AMF in experimental animal models. These experiments were initially hindered by a substantial and previously unsuspected species preference (about 100 fold for mouse versus human AMF). When administered to nude mice, CHO tumors constitutively over-expressing and secreting mouse AMF caused periosteal (on the outer surface of the long bones) new bone formation -an osteoblastic response, similar to the type which is found with about 15% of breast cancers metastatic to bone. In the past year we found that this periosteal response was consistent in two different models of metastasis. We also found that whenever the serum AMF concentrations of tumor-bearing animals were significantly increased, the animals displayed tumor-associated weight loss (cachexia), a major cause of morbidity and mortality in advanced metastatic disease. We found the effects of AMF on bone to be independent of the factor PTHrP, which we have previously shown plays a central role in osteolytic bone metastases caused by breast cancer. The elucidation of the interrelationship between PTHrP and AMF was a major goal of this proposal. We also have determined the clearance rate of AMF from the mouse circulation.

The species-specific effects of AMF remain little understood; so we have undertaken to clarify the stucture:function relationships involved. In the past year we cloned, sequenced and expressed rabbit AMF, for which the x-ray crystallographic data were already partially solved. These results have been published. We also developed a recombinant protein expression system for the mouse and human factors, which we are now able to prepare in 100mg batches. The human factor has been successfully crystallized and the x-ray structure solved to 1.8Å by our collaborator. Sequences of the putative receptors for AMF from mouse and human cells were described 6 months ago; so it will now be possible to study ligand:receptor interactions.

BODY

For the sake of clarity, the tasks completed in the first year of this award are briefly summarized. Then those completed during the second year (the subject of this progress report) are described. Finally the tasks remaining for the third year ahead are listed. The task numbering used is that of the statement of work (SOW) in the original proposal. The original proposal included 48 references. We continue this numbering with references added here beginning at 49.

1) Progress in first year (previously reported) 1: Tasks 1-3, the analyses of secretion of AMF by various breast cancer cell lines, effects of exogenous factors on AMF secretion by cancer cells and on growth rates were completed on schedule. Unfortunately the regulation of AMF secretion (which goes via an entirely unknown, non-classical pathway) remains mysterious. Since it is not understood in vitro, we still have no idea how it might be regulated in vivo from tumor cells. R Kumar's laboratory recently reported regulation of AMF expression by heregulin (49); however this work did not demonstrate changes in secretion of functional AMF from the cells.

Tasks 4 and 5, initial animal experiments, have been completed. The results of 5) are reported in the next section. Task 6, the preparation of a CHO cell line producing both mAMF and PTHrP and its use in the animal model (tasks 7-9, which were scheduled to overlap from years one into two)) has been completed. The results are summarized in the following section. Task 10, construction of amplifiable AMF plasmid was completed. This was intended for use in task 11 in year 2. This overall strategy has proven unsuccessful (discussed in the next section); so we present in the third section, alternate strategies now underway to carry out task 11. Tasks 15 and 16, data analyses and preparation have been carried out routinely in each year, as originally proposed.

2) Current progress (4/1999-4/2000):

Effects of AMF on bone metastases in vivo (tasks 4-9). We tested the effects of mouse AMF overproduction in nude mice using the CHO-1C6 cell line, which constitutively overproduces AMF from a gene-amplified plasmid vector. Conditioned media from this cell line have 8 fold elevated AMF content (80ng/ml/48hrs/million cells) compared to the control CHO-K1 cell line, in the absence of cell lysis, which releases intracellular PGI. All methods were as described in the original proposal.

A) Effects of AMF overproduction by intramuscular tumors. The CHO-1C6 (AMF+) tumor line grows slightly faster both in vitro and in vivo than the CHO-K1 control. When these two cell lines were inoculated into the thigh muscle of nude mice, all animals developed large IM tumors. The periosteal bone surfaces of those mice bearing AMF+ tumors showed new bone formation by x-ray (**figure 1**, reported previously), indicated by arrows on the center and right-hand panels, compared to the mice bearing control tumors (left hand panel). This was confirmed by histology of bone sections following fixation and decalcification (**figure 2**). The arrows on the right hand panel indicate new bone formation

on the surface of the femur adjacent to the site of growth of the AMF+ CHO-1C6 tumor. We detected no such periosteal osteoblastic response in the the control CHO-K1 tumor-bearing animals. All animals were examined at autopsy and showed no tumor at other sites.

The tumor-bearing animals were assessed for body weight, whole blood ionized calcium, and for plasma AMF concentrations. By assay of AMF via its phosphoglucose isomerase activity, we are readily able to detect basal AMF activity from 10µl of serum. In these experiments (with 6-8 animals per group) all the animals remained normocalcemic (**figure 3**), while plasma AMF was elevated in the AMF+ group only **figure 4**), and body weights were significantly decreased in the AMF+ group only (**figure 5**) compared to controls. [Please note that the experimental milli-units of PGI activity in figure 4 correspond to 1ng of 125Kda dimeric AMF protein.] Significance was determined by ANOVA. This experiment and the following one were halted at 2-3 weeks after cell inoculation, when the AMF+ animal groups showed severe cachexia and paraplegia.

B) Effects on AMF overproduction by tumor cells metastatic to the long bones. The same experiment as the previous one was carried out, except that the mice were inoculated with the two types of CHO cells by the intracardiac route, which results in rapid development of osteolytic lesions, visible by x-ray, in the long bones near the growth plates. These animals did not have significant tumor formation at non-bone sites. The lesions on the primary x-rays (not shown) were quantified by a blinded observer using a computerized image analysis system. The results are expressed as both lesion number and lesion area (**figure 6**). AMF over-expression decreased both of these parameters compared to the lesions seen with the CHO-K1-bearing control animals; however, this reduction did not reach statistical significance and may reflect a trivial explanation due to the slightly slower growth rate of the AMF+ cell line. Very surprisingly, the detailed histological analysis of the bones from this experiment showed periosteal new bone formation indistinguishable from that seen with the intramuscular tumors in the previous experiment. **Figure 7** shows representative results. The left hand panel shows a normal bone free of tumor. Cortical bone is intact, surrounding a marrow cavity containing trabecular bone and normal marrow cells. The right hand panel shows a bone with a severe osteolytic metastasis caused by the CHO-K1 control cell line. The tumor has completely replaced the marrow cavity, destroying the trabecular bone and eroding through the cortical bone at the upper right; so that tumor is now growing outside of the bone shaft. This same phenomenon is seen in the center panel with the AMF-overproducing CHO-1C6 cell line. However, the osteolytic metastases in the animals, after erupting through the cortical bone, caused periosteal new bone formation (indicated by the arrow in **figure 7**) where the erupted tumor is in contact with the external surface of the long bone shaft. We have not been able to perform quantitative histomorphometry of the periosteal new bone formation, since there is normally no such bone formation at this site. There is therefore no baseline to which the experimental values could be compared. The new bone formation was consistently seen in all animals carrying well-advanced AMF+ tumors adjacent to the periosteum.

The histological results indicate that cells on the periosteum of bone, but apparently not on the inner surface of bone (either covering the trabecular elements or lining the inner aspect of the cortex) are specific targets for the effects of tumor-produced AMF. It is observed that breast cancers metastatic to bone result in about 85% osteolytic response and 15% osteoblastic, whereas bony metastases from prostate cancer are more often osteoblastic (1,2). It was our hypothesis when this proposal was submitted that AMF was probably an osteolytic factor and hence likely to be synergistic with PTHrP: the basis of the experiments in tasks 6 and 11 in particular. However, it now appears that AMF is, among other things, an osteoblastic factor. Our results show that it is an important factor causing pathological alterations in bone when the factor is expressed by metastatic tumor cells adjacent to bone.

The animals in this experiment were assayed, as before, for serum AMF concentration, whole blood ionized calcium, and body weight. All animals remained normocalcemic (not shown). Both groups showed equivalent weight loss and serum AMF activity increases (**figures 8 and 9**). It should be noted that the assay used for AMF cannot distinguish host animal (mouse) from tumor-derived (human) AMF. We are unaware of any currently available reagents (such as monoclonal antibodies) which would permit this species-specific distinction. [Please note that, as above, the experimental milli-units of PGI activity in figure correspond to 1ng of 125Kda dimeric AMF protein.]

Our previous data (contained in the progress report for last year) showed species-specific effects of AMF, suggesting that biologically active AMF in the osteolytic metastasis experiments is likely to be the mouse factor (and thus host-derived). They also suggest a biphasic dose-response of target cells to the factor; so that only intermediate levels of the factor (around 1ng/ml) are likely to be agonistic. Finally, we previously showed that one of the effects was not directly upon osteoclasts or their precursors, but via the modulation of gene expression (such as RANK ligand and osteoprotegerin) of bone marrow stromal cells. These cells are in the osteoblast lineage; so it is not unreasonable to see an osteoblastic response from cells that bind AMF. It is only in the last six months that the full, correct sequences of two cDNAs have been published which probably encode the mouse and human AMF receptors (50). These closely related sequences encode a new subfamily of 7-transmembrane domain G-protein-coupled receptors, with a small N-terminal extracellular domain and a very large C-terminal cytoplasmic domain. Formal proof has not yet been published that these proteins are capable of high affinity binding to AMF ligand proteins and transduction of signaling responses to exogenous AMF. The published data indicate that the putative AMFR is abundantly expressed by all mouse tissues tested except for spleen. We inspected the mouse and human EST database and found that the putative receptors are widely expressed in these databases, with over 100 hits for each species. We have prepared a nearly full-length mouse AMFR cDNA clone in a mammalian expression vector and are isolating a human cDNA.

C) Interactions between AMF and PTHrP in vivo. The data in the previous section indicate that, contrary to our original hypothesis, AMF does not act as an osteolytic factor in bone metastases. Thus, synergistic or additive interactions between these two factors, AMF and PTHrP, were no longer anticipated (the purpose for tasks 6 and 11). We nevertheless were puzzled and surprised by the osteolytic phenotype displayed by both

control and AMF+ CHO cells in the previously described experiment. We therefore tested whether these cells might express endogenous PTHrP. The cells are of ovarian origin, and ovary is one of a number of tissues reported to express PTHrP. PTHrP was determined by Nichols 2-site ELISA of serum free medium conditioned for 48 hours by CHO-K1 and CHO-1C6 cells, with and without treatment with TGFbeta (a potent inducer of expression of PTHrP by breast cancer cells, ref. 51). **Figure 10** shows the surprising result that both cell lines express substantial amounts of PTHrP. The receptor-binding N-terminus of PTHrP is identical in most mammals, and Chinese hamster PTHrP should have biological activity identical to either mouse or human factor. The level expressed by the two CHO cell lines is higher than that from unstimulated MDA-MB-231 breast cancer cells (51) and sufficient, from our experience to cause, osteolytic metastasis without systemic hypercalcemia. The CHO PTHrP was not regulated by TGFβ. We have tested several other CHO cells lines expressing recombinant factors, and not all are PTHrP+. Thus, in this experiment we unintentionally completed tasks 6-9. The results from this task rendered task 11 entirely irrelevant. Below, we propose a modified version of task 11 and the subsequent tasks dependent upon it.

D) Species-specific effects of AMF. Our data from the first year with osteoclast formation in bone marrow cultures showed a strong selectivity for the mouse factor with mouse cells and human factor with human cells. We are not aware that this ~100X species specificity has been observed in other assays. Two recent papers from an x-ray crystallography group in Taipei have reported that PGI/AMF from *Bacillus stearothermophilus* has AMF and neuroleukin biactivities in mammalian cell assays (51,52). These data were reported without full controls, statistical analysis for significance or characterization of the bacterial protein (such as freedom from endotoxin contamination). We are thus unconvinced that bacterial protein has AMF biological activities and were prompted to pursue basic biochemical characterization of the structural and functional bases of AMF activity in our bone cell assays in vitro. We therefore formulated a new task: **Additional Task 17: Preparation of pure recombinant AMFs from multiple species**. At the time we began this new task (summer 1999), data on the structures of mammalian PGI/AMFs were unavailable at high resolution. Conversations with Dr Christopher Davies, an x-ray crystallographer at University of Sussex, Brighton UK, indicated that x-ray data on the rabbit muscle protein were incompletely interpretable due to lack of the primary amino acid sequence. Our preliminary data for this proposal were obtained with rabbit muscle protein as a surrogate for the commercially unavailable human protein. We therefore undertook an efficient molecular approach to obtaining the cDNA sequence or rabbit AMF without the need to screen a cDNA library, based on highly conserved regions within the published sequences of mouse, human, and pig cDNAs. This strategy was fully successful, and the results have been published. The sequence is now publically available from Genbank (53). At the same time the laboratory of Petsko solved the rabbit x-ray structure and obtained the same cDNA sequence (54).

As part of our cloning strategy, rabbit AMF was modified by PCR mutagenesis to create a 1.7kb DNA fragment flanked by unique Nde I (in frame with the initiator methionine codon) and EcoR I sites. The C-terminus was modified to add six consecutive

His codons followed by a stop codon. The 6His extension allows facile one-step purification by affinity chromatography under native conditions on NiNTA agarose. All of the technical details are provided in ref 53, a copy of which is appended. The Nde I to EcoR I DNA was subcloned into the commercially available bacterial T7 expression vector pET5a and introduced into E coli strain BL21DE3pLysS. Induction with 0.3mM iPTG resulted in abundant soluble expression of PGI/AMF. Again, all details are published. At the same time, we identified IMAGE clones encoding mouse and human PGIs from the Genbank EST databases. These clones were used to generate parallel Nde I to EcoR I fragments encoding 6His-tagged versions of both mouse and human AMFs (designated mAMFH6 and hAMFH6). These were expressed in E. coli and purified on NiNTA agarose. **Figure 11** shows a representative induction on independently isolated bacterial colonies carrying pET5a-mAMFH6. The prominent band just below the 62kDa molecular weight marker is the predicted size for mammalian AMF/PGI (558 amino acids without the 6His extension). The rabbit, mouse, and human 6His proteins have all been expressed in E. coli and purified to >95% homogeneity by a single step binding to Qigen NiNTA agarose and elution with 0.25M imidazole. Yields are 30-70mg pure protein per liter of bacterial culture after 3hrs induction at 30°C. Each protein showed a single band of about 60kDa on reducing denaturing SDS PAGE gel followed by Coomassie blue staining (**figure 12** shows representative purification for mouse AMFH6). The proteins were characterized for PGI activity by conventional steady state kinetic assays and showed Km and Vmax values similar to one another and to those published for the enzyme conventionally purified from rabbit muscle. Mouse and human proteins were sent to Dr. Davies in Brighton and have yielded good quality crystals. Dr. Davies has recently solved the crystal structure of human AMF125kDa dimer to 1.8Å resolution (personal communication), using this recombinant material. We assayed the recombinant mAMFH6 and hAMFH6 for endotoxin contamination using a Limulus amoebocyte assay kit from Sigma. LPS contamination was less than one part per thousand. We tested these same two protein preparations in the bone marrow osteoclast differentiation assay described in the original proposal. **Figure 13** shows that mAMFH6 has potent biological activity at 0.1ng/ml (approximately 1pM) in the mouse marrow culture assay. As seen before, the dose-response curve was bell-shaped. As found previously, very much higher concentrations of human AMF were required for a significant response in this assay (**figure 14**).

The results with bacterially expressed recombinant mouse and human AMFs fully confirm our previously reported results. They demonstrate that the biological activity of AMF on bone cells is not dependent on any mammalian post-translational modification or co-purifying contaminant. They provide an abundant source of the mammalian factors from three different species. They have also already provided the material for the solution of the crystal structure of human AMF. This new task was envisioned, designed, and completed entirely between the previous and the current progress reports.

3) Work to be undertaken during third year of project.

In the original proposal work in the third year included part of task 11 and tasks 12-14: to examine the effects in the mouse model of bone metastasis of over-expression of

AMF by the human breast cancer cell line MDA-MB-231. We showed in the work of this past year that AMF is an osteoblastic rather than an osteolytic factor and that its actions on bone are independent of those caused by PTHrP. We have already shown that the metastasis to bone of the MDA-MB-231 cell line is primarily dependent on PTHrP and its induction by bone-derived TGFbeta (7,8,55). Therefore there is no point in carrying out the precise experiment originally proposed. However, we believe that a very similar experiment merits performance. This would be to test in the mouse model of bone metastasis (exactly as proposed in tasks 12-14) expression of AMF in a relevant breast cancer cell line.

As discussed in the original application and above, the pathway by which AMF is secreted by cells is entirely unknown. It is therefore unclear how to manipulate cells to enhance their secretion through the nonclassical pathway. This pathway is used by cells to secrete IL-1, FGFs 1 and 2, several of the cancer-associated galectins, platelet-derived endothelial cell growth factor (like AMF, PD-ECGF is the secreted from of an intracellular enzyme, as is autotaxin), and clotting factor XIII A chain pro-transglutaminase (16,17). At least three proteins on this list (IL-1, FGF-2, and fXIIIA) have been successfully secreted from eukaryotic cells by providing their cDNAs with conventional ER signal peptides. We propose to test this approach. Two possible pitfalls are: a) the secreted AMFs will probably be glycoproteins and b) the relatively oxidizing environment of the endoplasmic reticulum may result in aberrant folding and disulfide bond formation involving the 3 to 5 free cysteine residues per AMF subunit. Aberrant folding is likely to result in the commonly encountered phenotype of ER retention and subsequent tetra-ubiquitin-mediated targeting to the proteasome for intracellular degradation.

As described above, mouse, human, and rabbit AMF cDNAs have been subcloned as parallel Nde I to EcoR I 1.7kb fragments which add 6His C-terminal extensions. The Nde I recognition sequence is CTA ATG, with the second half encoding the initiator methionine. We have prepared a 75 base PCR fragment which encodes the 20 amino acid ER signal peptide from a mouse IgG kappa light chain as a Hind III to Nde I restriction fragment, with the Nde I in the same reading frame as in the AMFs. This fragment will be ligated into the standard expression vector pcDNA3 cut with Hind III to EcoR I, along with the Nde I EcoR I fragments from the three species. DNAs will be checked by restriction mapping and tested by transient transfection into human HEK 293 cells. Serum-free conditioned media will be tested for expression of AMFH6 protein by binding to NiNTA agarose, elution with imidazole and SDS PAGE gels followed by silver staining for the expected 62kDa band. Activity will be tested by conventional PGI activity assay.

AMFs from all three species could be N-glycosylated at N91FS and N105RS. Mouse has an additional acceptor site at N39FS, and the human a third site at N249TT. If in these experiments no protein secretion is detected, the strategy will be terminated. If inactive protein is secreted, we can eliminate the 2 glycosylation sites by mutagenesis in vitro of the rabbit sequence for example. We have published these types of experiments previously. Standard protocols for renaturation in vitro of inactive PGI are available in the classic literature on the subject.

If the secretory strategy is successful, mouse and human pre-AMFH6s will be stably transfected into the MCF7 breast cancer cell line. MCF7s form bone metastases when inoculated by the intracardiac route (T Guise and T Yoneda, unpublished). The cells cause indolent osteoblastic or mixed lytic/blastic metastases, in the absence of PTHrP production.

Stable transfectants are readily made in MCF7s and will be screened by assay of conditioned media for PGI enzymatic activity.

Two other alternative approaches are available. One is parallel to the above but not as directly relevant. We now have available a bicistronic expression vector which carries the light and heavy chains for the monoclonal mouse IgG antibody 3F5, which we previously have used to neutralize PTHrP in vivo (55). This DNA (**Figure 15**) could be used stably to transfect the CHO-1C6 cell line to eliminate its production of active PTHrP in vivo. We have already shown that the DNA produces secreted nuetralizing activity. The DNA was transiently transfected into 293 cells and the IgG purified from serum-free conditioned media by binding to Protein G agarose. Eluted and neutralized material effectively inhibited Ca45 release from labeled neonatal rat long bones in response to exogenous synthetic PTHrP 1-34 (**figure 16**). PTHrP has nuclear, intracrine growth promoting effects at least in prostate cancer cells; so that the use of PTHrP-antisense DNA results in growth arrest of transfectants (our unpublished observations with the PC3 prostate cancer cell line.) The antibody secreting plasmid approach will neutralize only the PTHrP secreted outside the CHO cells, providing a reasonable surrogate of the originally proposed experiment.

A final alternative is to use our now readily available recombinant mouse mAMFH6 in animals. We have tested this material by ip injection (**figure 17**), resulting in readily detectable increases in the assayed levels of AMF in the peripheral circulation. These results indicate that AMF is rapidly cleared from the bloodstream. A multi-week bone metastasis experiment would require an impractical number of injections every few hours to sustain elevated blood levels. We are presently investigating the practicality of using Alzet minipumps to deliver the active factor. We do not yet have a detailed protocol for this experiment but will provide one prior to initiating such as approach. This technology would permit us to test the effect of AMF alone on systemic responses, such as cachexia, and on the fate of injected MCF7 cells to metastasize to bone.

4) Future Directions.

We think it likely that AMF could play a systemic role in cachexia of malignancy, which accompanies virtually all advanced cancers and which we have observed to be invariably associated with advanced bone metastases in the animal model. These same animals always have raised plasma AMF concentrations (**figures 4 and 9**), which is consistent with the old literature on PGI as a marker of human metastatic breast cancer tumor burden (18,19). We have tested whether the sera of the mice assayed in figures 4 and 9 had increased concentrations of several well-known cachectic factors. The samples were assayed with ELISA kits from R&D Systems for mouse IL-6 and mouse TNFα. Neither factor was present above the limits of detection (60pg/ml and 30pg/ml, respectively). Other cachectic factors, such as IL-1, have not been assayed. The availability of the recombinant AMF proteins will permit testing of whether AMF itself is a cachectic factor in mice. The 6His tags will provide a means of distinguishing exogenous from endogenous AMF in experimental animals. We are obtaining (not with Army funds) a panel of mouse monoclonal hybridomas against hAMFH6, which has proved to be an excellent immunogen in mice.

The AMFs from mouse and human are 88% identical and have a number of conserved unique restriction sites; so that it would be straightforward to generate mouse-human chimeric AMF proteins and purify them from E. coli. These would allow us to determine the structural basis of the species-specific binding, which we presume to be via binding to the mammalian AMFRs. The species-specific receptor:ligand interactions could provide future targets for pharmacological intervention to block effects of tumor-produced effects on bone and on cachexia.

Publications: The first paper from this work was published earlier this year (53). Data collection is complete and we anticipate submission of three papers this year: One ,on effects of AMF on RANK ligand, osteoprotegerin, and osteoclastogenesis in vitro. Two, on the effects of mouse AMF to cause perisoteal new bone formation iv vivo. [These data have been selected for oral presentation at the European Society for Calcified Tissue Research meeting in Tampere Finland , May 2000]. Three, describing the expression, purification, and kinetic and biochemical characterization of this AMFH6s from mouse rabbit and human and the activity of the recombinant mouse protein on bone cells in culture.

figure 1

LOCAL EFFECTS OF AMF ON BONE

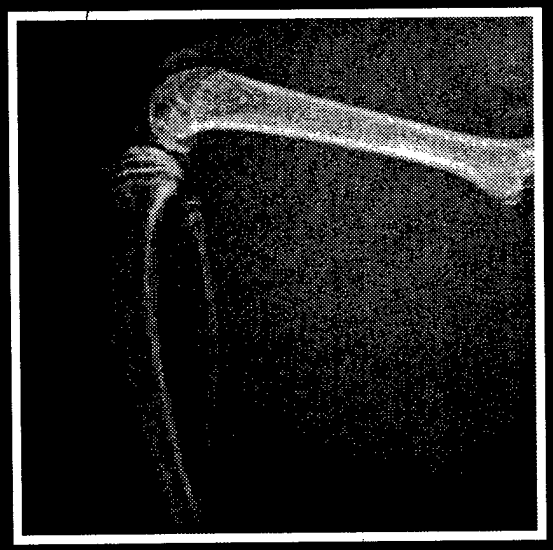

CHO CONTROL

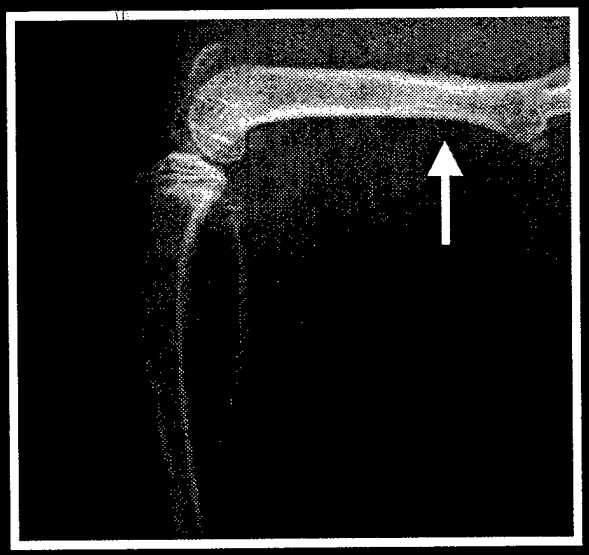

CHO/AMF

CHO/AMF

figure 2

figure 3

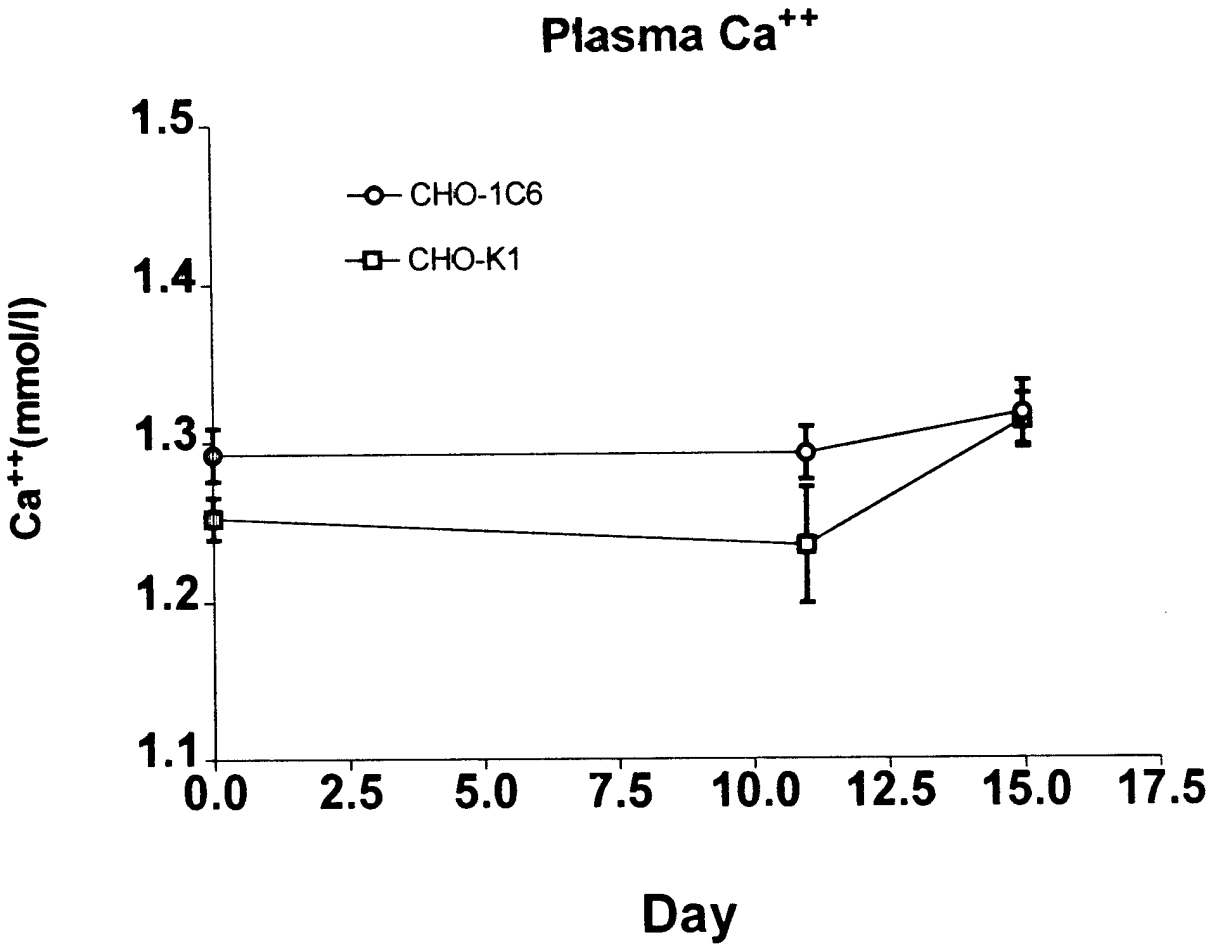
Plasma Ca++
1.5
1.4
1.3
1.2
1.1
Ca++(mmol/l)
CHO-1C6
CHO-K1
0.0
2.5
5.0
7.5
10.0
12.5
15.0
17.5
Day

figure 4

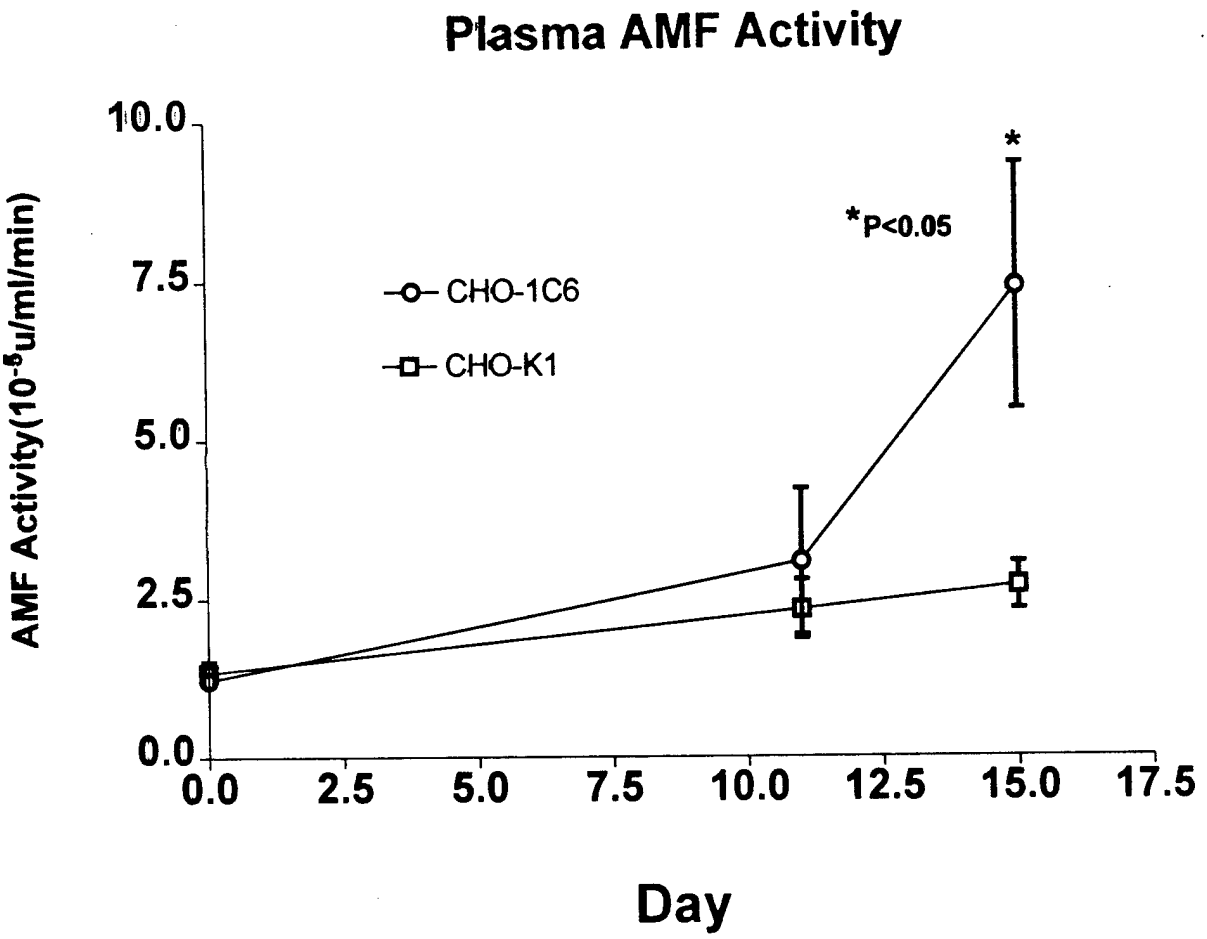
Plasma AMF Activity
AMF Activity(10^{-5}u/ml/min)
10.0
7.5
5.0
2.5
0.0
*P<0.05
CHO-1C6
CHO-K1
0.0
2.5
5.0
7.5
10.0
12.5
15.0
17.5
Day

figure 5

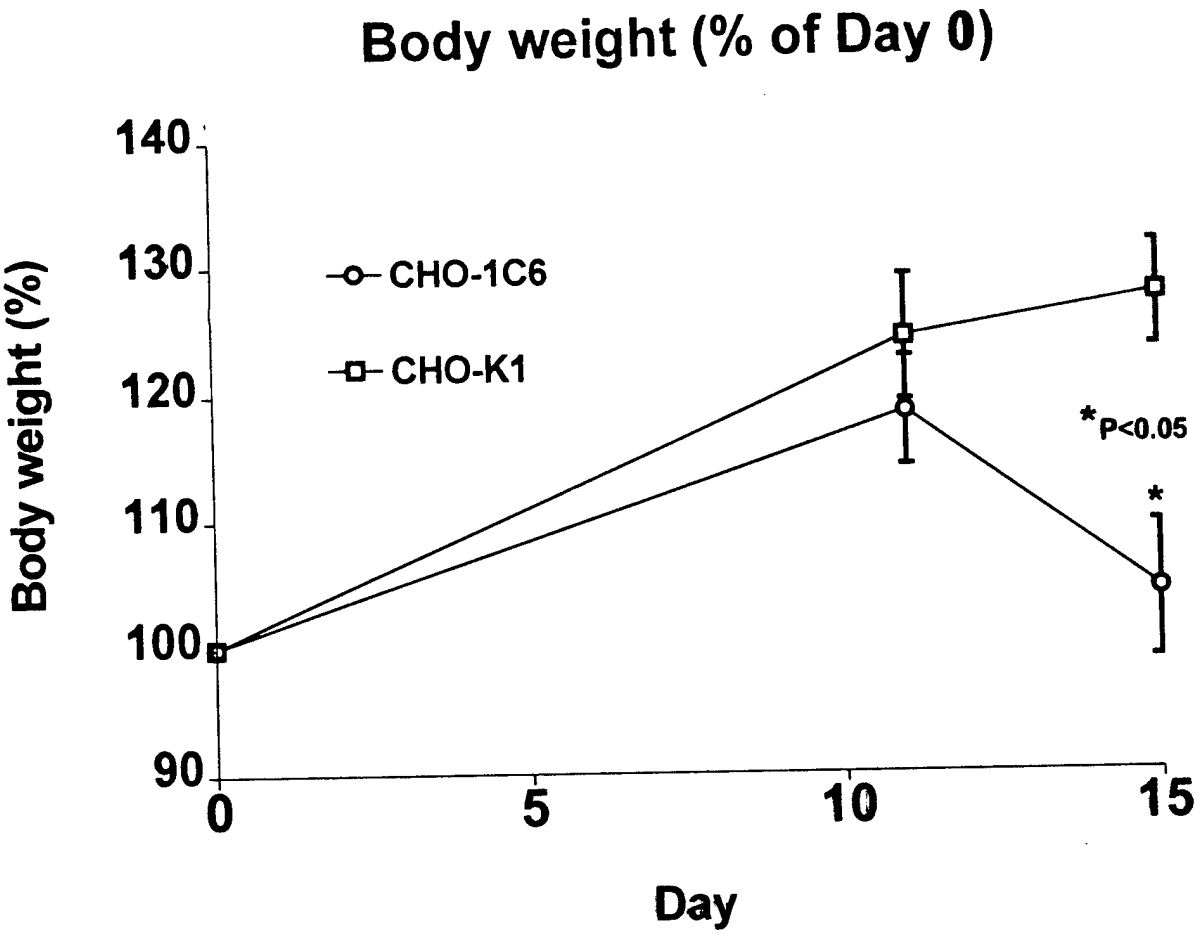
Body weight (% of Day 0)
Body weight (%)
140
130
120
110
100
90
CHO-1C6
CHO-K1
*P<0.05
*
0
5
10
15
Day

figure 6

Effect of CHO-K1 / CHO-IC6 on long bone osteolytic metastases

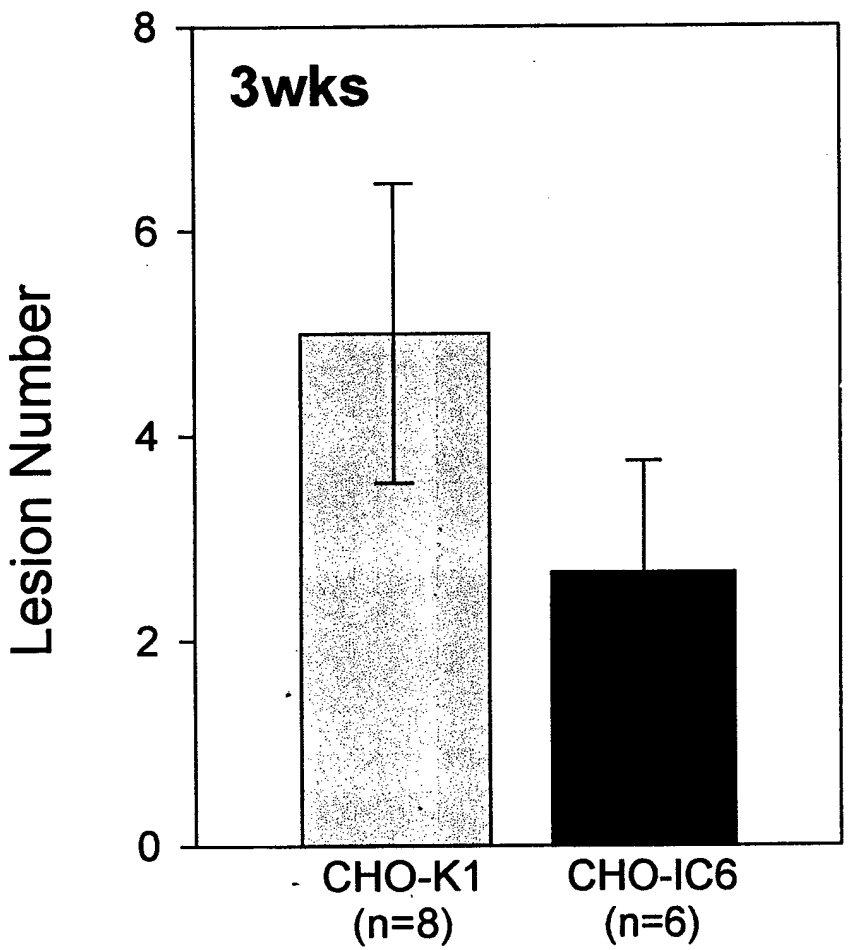

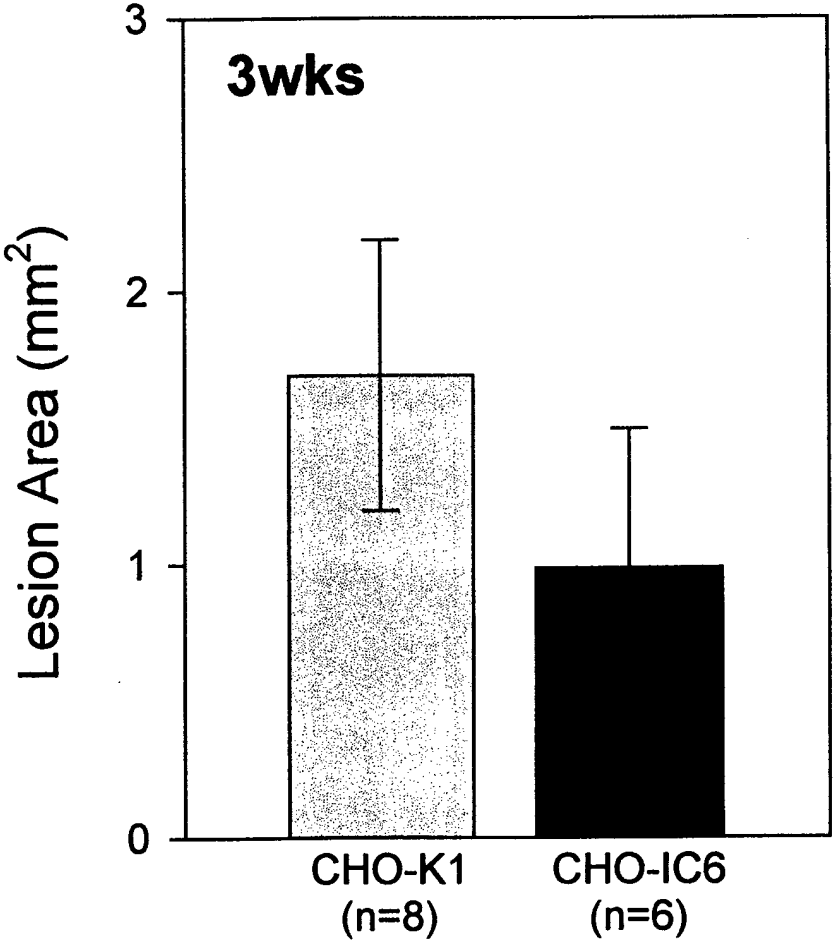

04/09/99

figure 7

EFFECTS OF AMF ON BONE METASTASIS

NO TUMOR

CHO/AMF

CHO CONTROL

figure 8

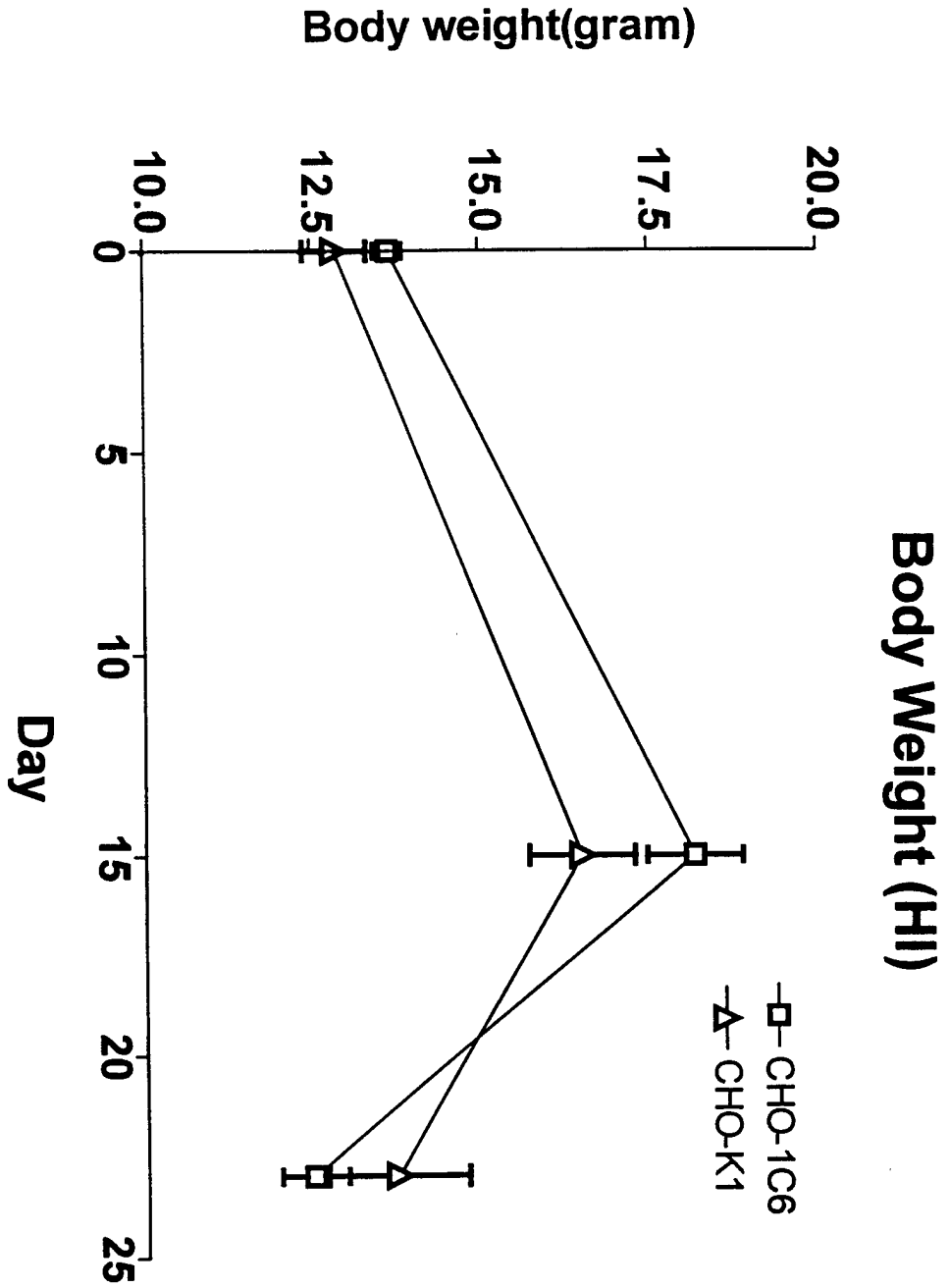
Body weight(gram)
20.0
17.5
15.0
12.5
10.0
0
5
10
15
20
25
Day
Body Weight (HI)
CHO-1C6
CHO-K1

figure 9

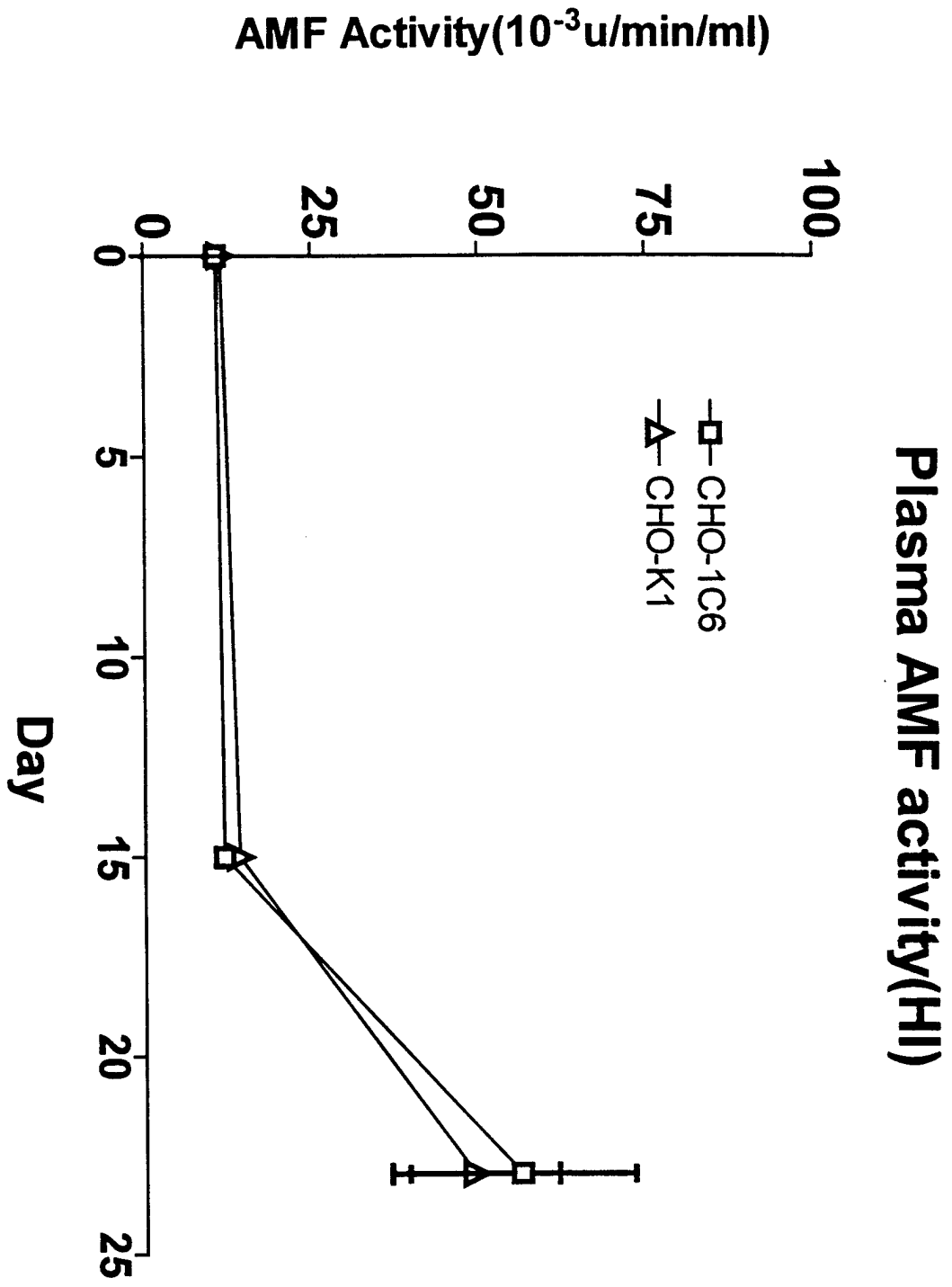
AMF Activity(10^{-3}u/min/ml)
Plasma AMF activity(HI)
CHO-1C6
CHO-K1
Day
0
25
50
75
100
0
5
10
15
20
25

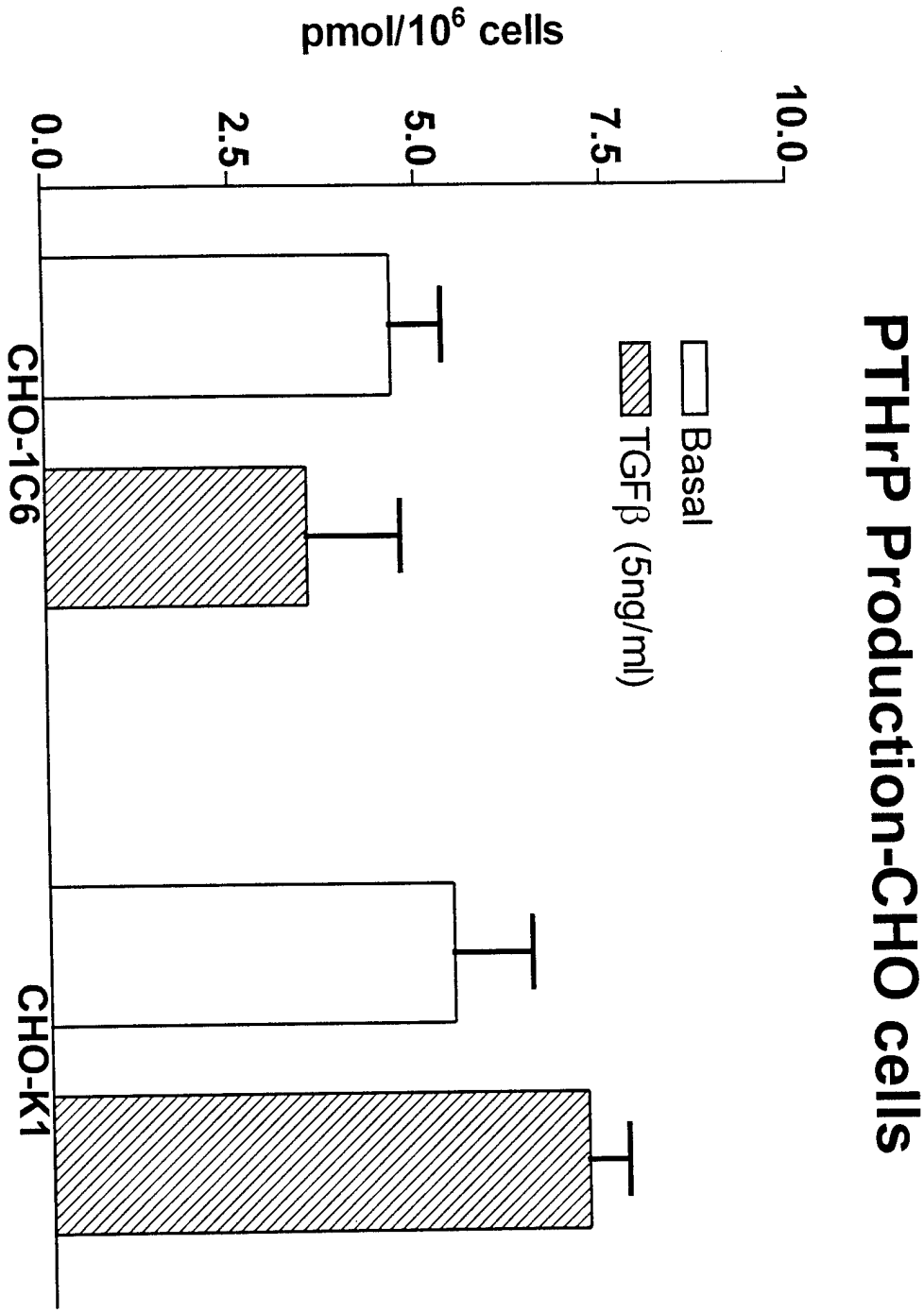
PTHrP Production-CHO cells
pmol/10^6 cells
0.0
2.5
5.0
7.5
10.0
Basal
TGFβ (5ng/ml)
CHO-1C6
CHO-K1

figure 11

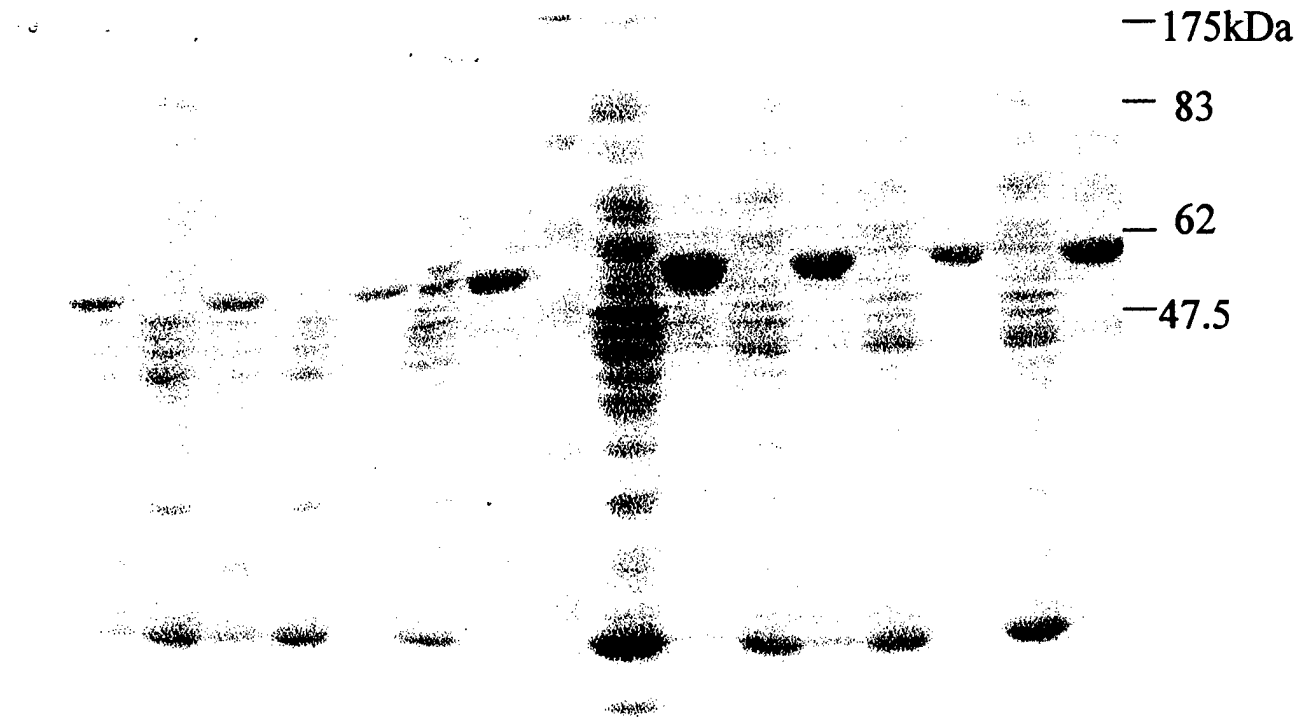

- Uninduced

+ Induced (IPTG 0.4mM)

figure 12

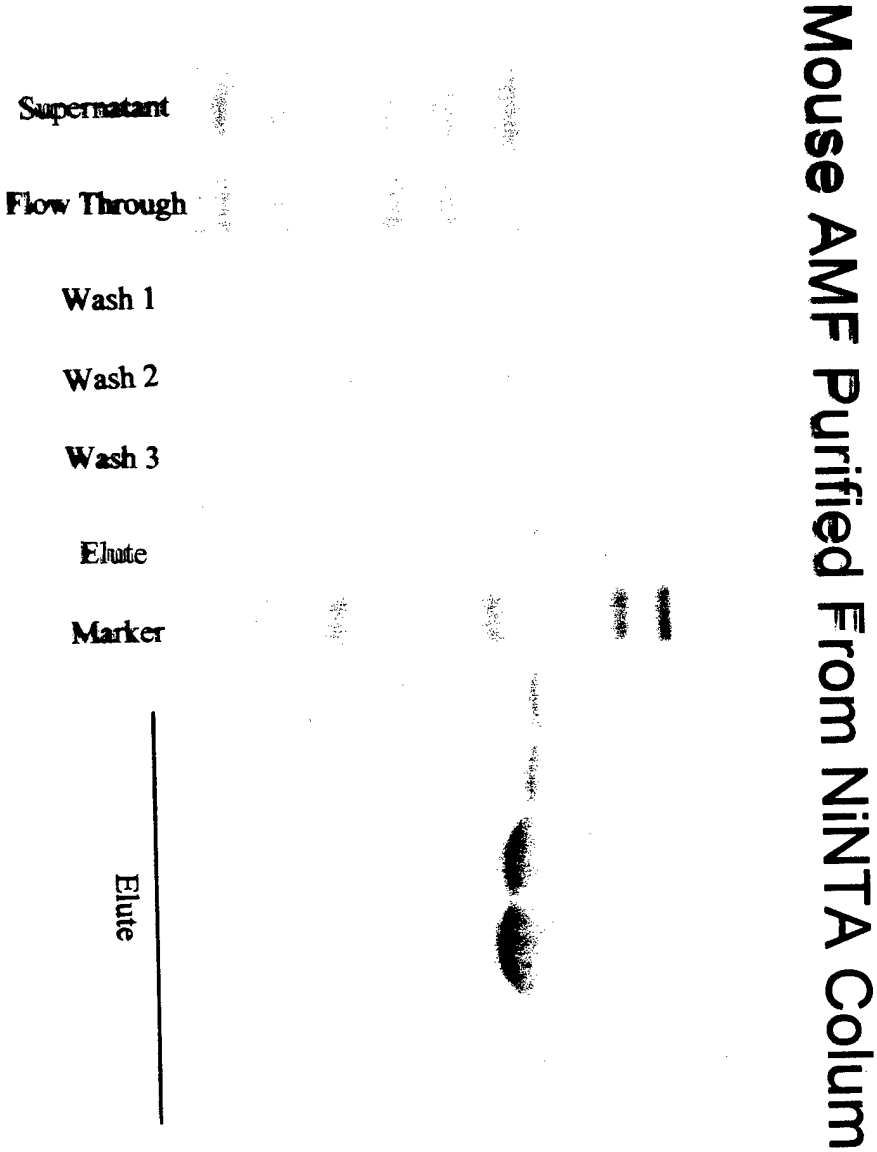
Mouse AMF Purified From NiNTA Column
Supernatant
Flow Through
Wash 1
Wash 2
Wash 3
Elute
Marker
Elute

figure 13

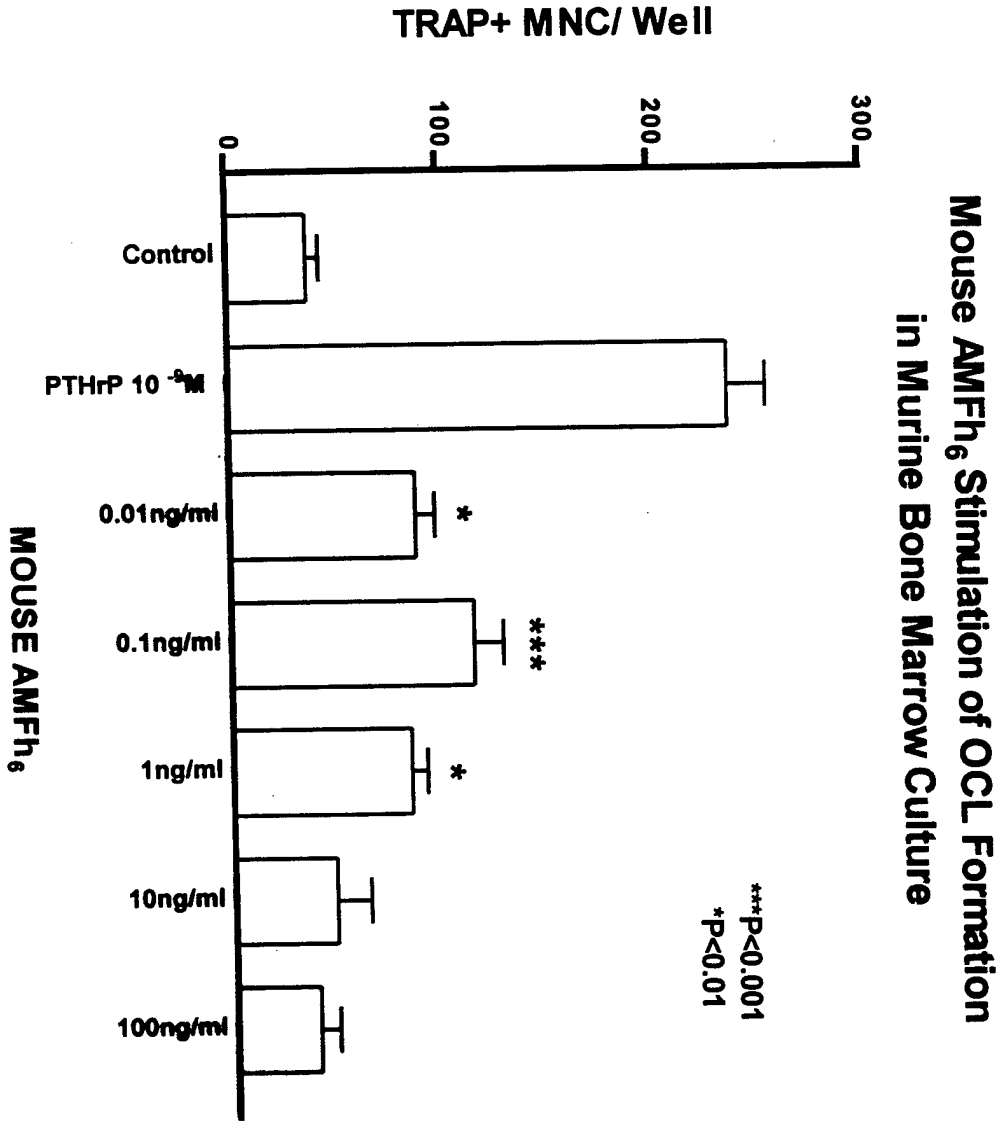

Mouse AMFh$_6$ Stimulation of OCL Formation in Murine Bone Marrow Culture

***P<0.001
*P<0.01

figure 14

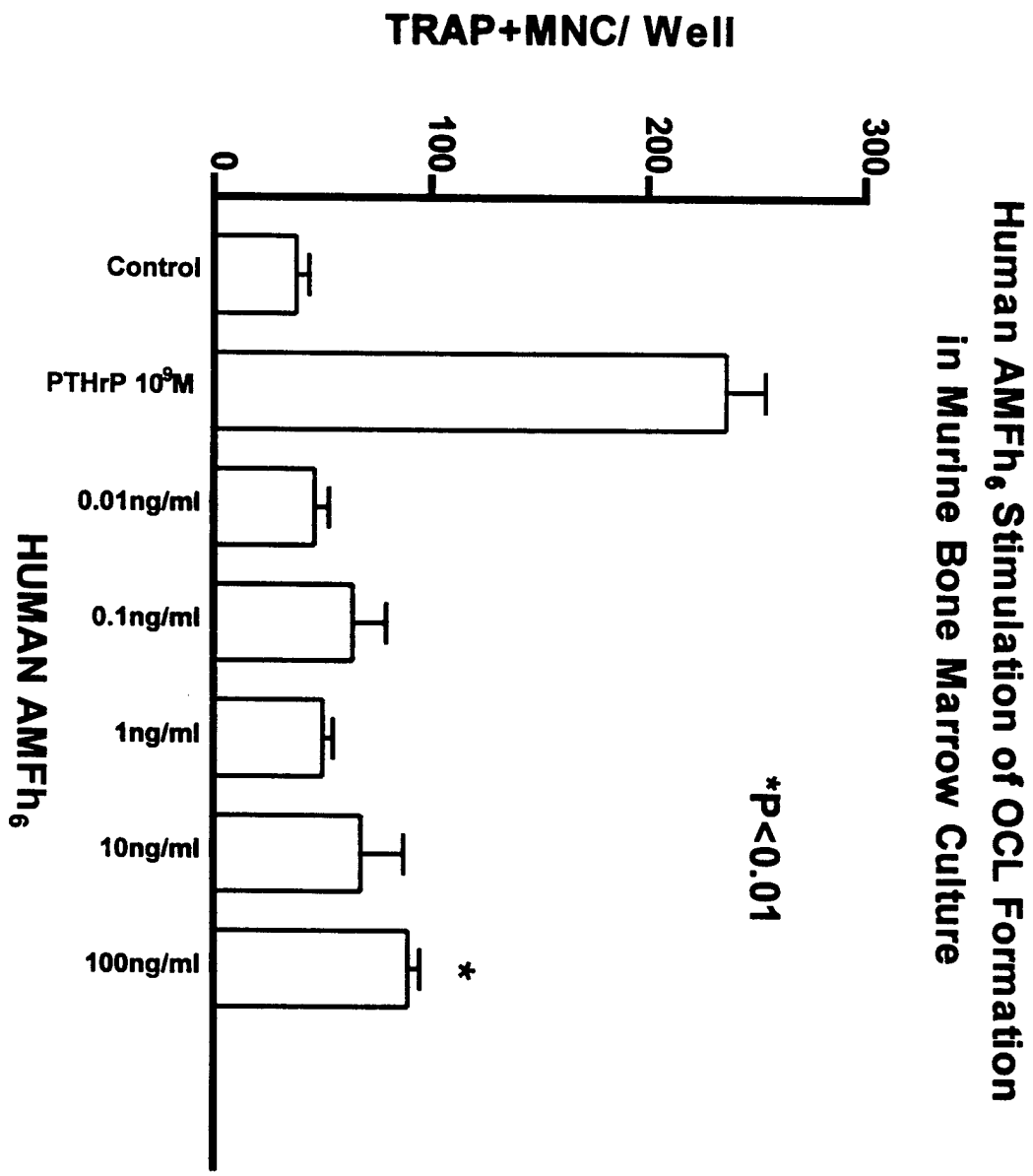
TRAP+MNC/ Well
0
100
200
300
Control
PTHrP 10⁻⁹M
0.01ng/ml
0.1ng/ml
1ng/ml
10ng/ml
100ng/ml
*
HUMAN AMFh6
Human AMFh6 Stimulation of OCL Formation
in Murine Bone Marrow Culture
*P<0.01

figure 15

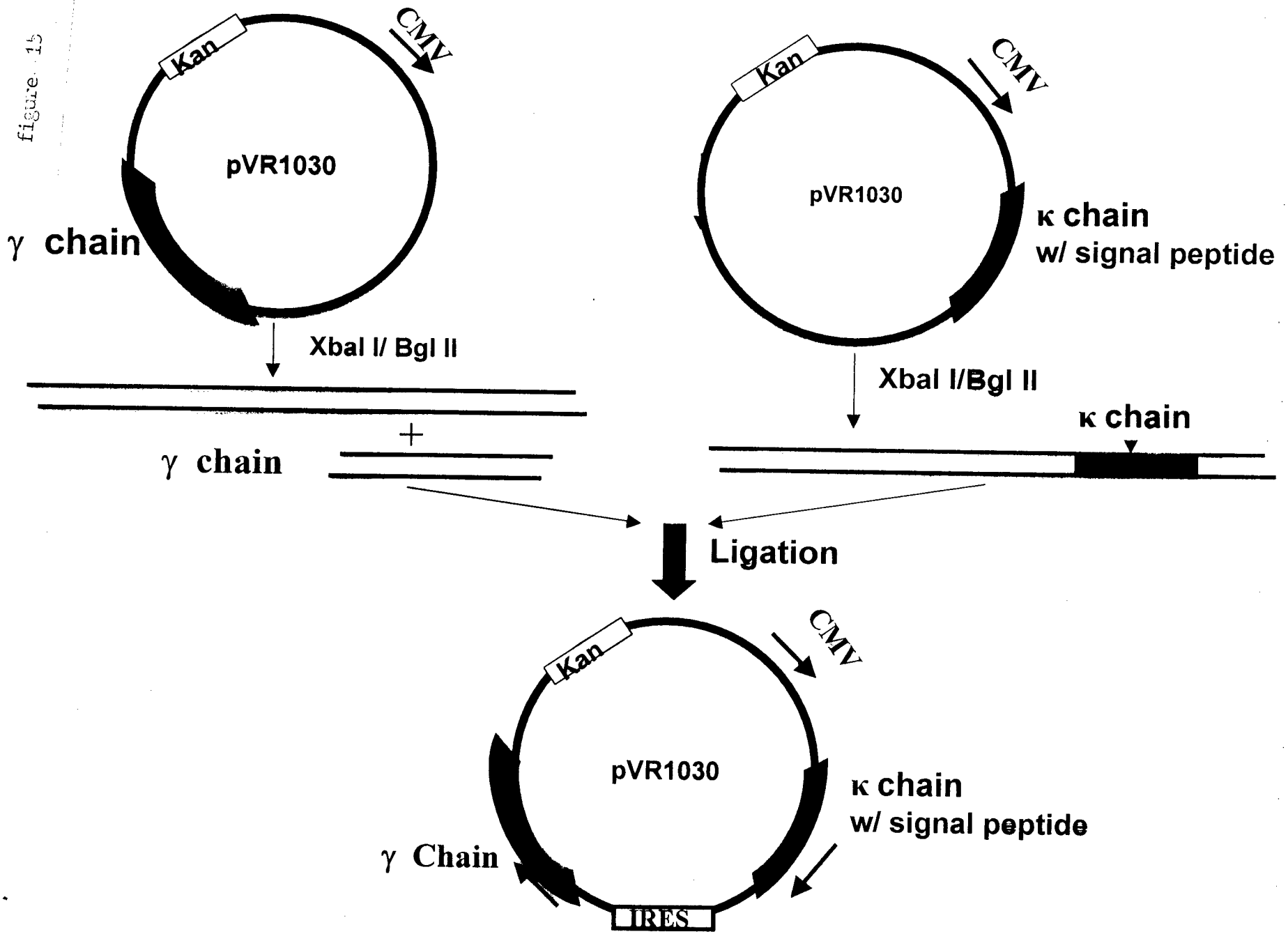
Kan
CMV
pVR1030
γ chain
Xbal I/ Bgl II
γ chain
+
Kan
CMV
pVR1030
κ chain
w/ signal peptide
Xbal I/Bgl II
κ chain
Ligation
Kan
CMV
pVR1030
κ chain
w/ signal peptide
γ Chain
IRES

figure 16

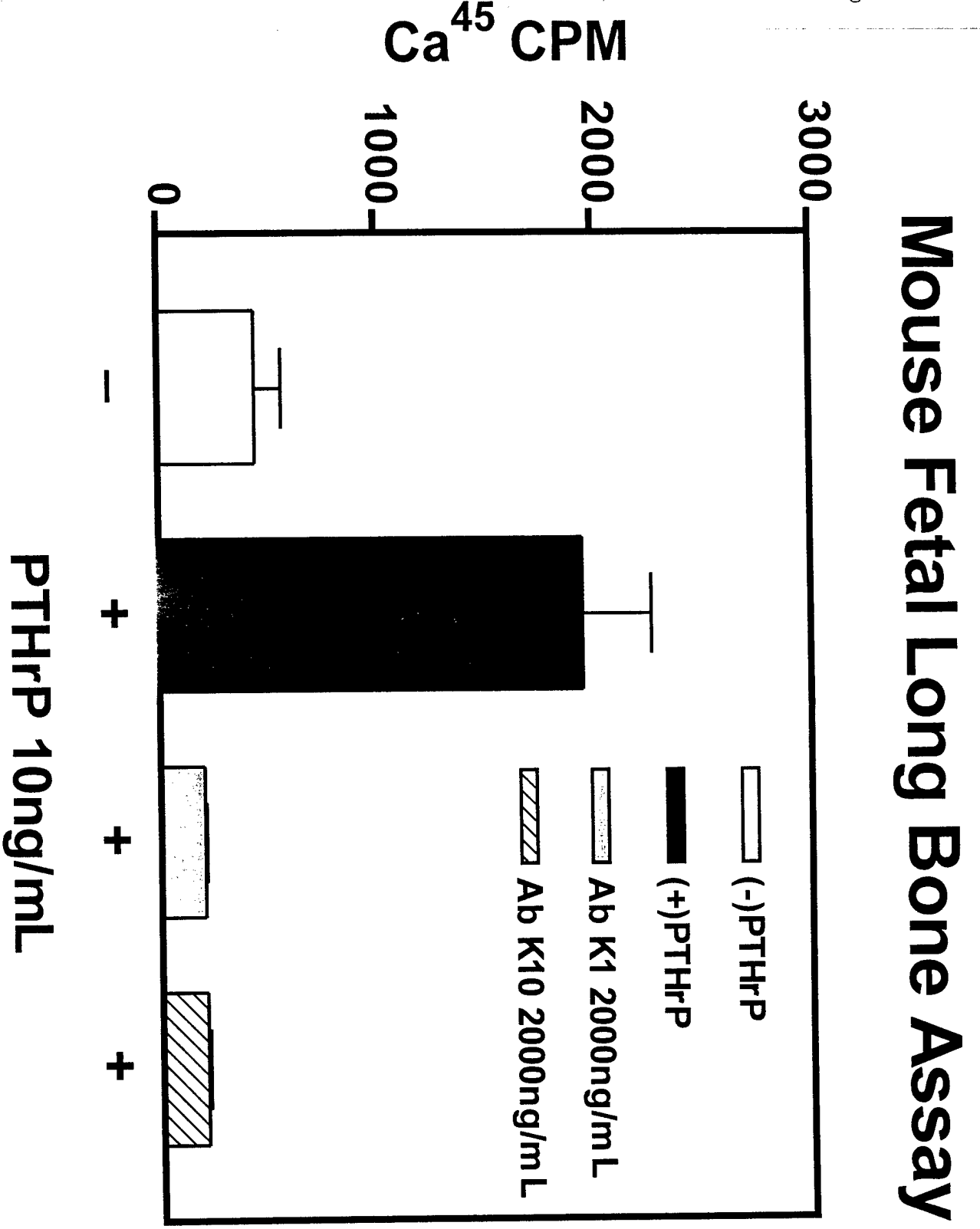
Mouse Fetal Long Bone Assay
Ca45 CPM
0
1000
2000
3000
(-)PTHrP
(+)PTHrP
Ab K1 2000ng/mL
Ab K10 2000ng/mL
PTHrP 10ng/mL
–
+
+
+

figure 17

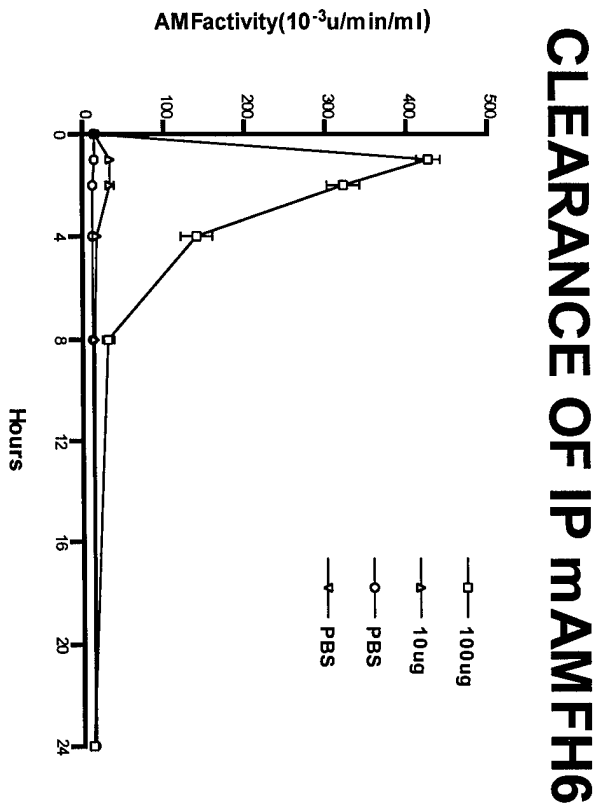
CLEARANCE OF IP mAMFH6
AMFactivity(10^{-3}u/min/ml)
0
100
200
300
400
500
Hours
0
4
8
12
16
20
24
100ug
10ug
PBS
PBS

KEY RESEARCH ACCOMPLISHMENTS

- AMF is a species-specific regulator or RANK ligand and osteoprotegerin mRNAs
- AMF induces mouse and human osteoclastogenesis in vitro

- **AMF induces periosteal new bone formation in vivo. This is the first animal model experimentation with AMF**
- **Effects of AMF are independent of the osteolytic factor PTHrP**

- **Rabbit AMF cDNA cloned, sequenced, expressed, and purified**
- **Mouse AMF cDNA cloned, expressed, and purified**
- **Human AMF cDNA cloned, expressed, and purified**
- **Recombinant mouse and human factors normally active on bone cells**

- **Serum AMF elevated ~4X in mice bearing AMF+ tumors**
- Serum AMF elevated ~4X in mice bearing bone metastases
- **Serum clearance rate of mouse AMF determined**

- **Mouse and human AMF proteins crystallized**
- **Structure of human AMF collaboratively solved to 1.8Å**

- **Serum [AMF] correlated with cachexia. Effects independent of IL-6 or TNFα**

Bold indicates established during the second year of the proposed work.

REPORTABLE OUTCOMES

First paper published:

X li, JM Chirgwin (2000). Rabbit phosphoglucose isomerase/neuroleukin/autocrine motility factor: cloning via interspecies identity. *Biochim Biophys Acta* **1476**: 363-367.

Abstract selected for oral presentation at the European Society for Calcified Tissue Research meeting in Tampere Finland , May 7, 2000:

X Li, SJ Choi, GD Roodman, TA Guise, JM Chirgwin. Autocrine Motility Factor (AMF) Stimulates Periosteal New Bone Formation.

CONCLUSIONS

AMF is a potent, multi-functional, biologically active, extracellular factor with unanticipated effects on bone when expressed by tumors metastatic to the skeleton. Effects are presumed to be mediated via recently-described seven transmembrane domain receptor class widely expressed on a variety of mammalian cell types (50). The biochemical basis of binding is as yet unexplored. Osteoblastic metastases are the second major type of breast cancer metastasis to the skeleton and the most common type of prostatic cancer metastasis to bone. AMF may play important roles in this important pathological and incurable complication of malignancy. Detailed biochemical characterization of the human and mouse factors, including their high resolution crystal structure, will facilitate understanding the molecular interactions of these potent ligands with their receptors. We have developed an abundant source of pure, active, recombinant factors which will greatly facilitate future work. We are now able to prepare mutant factors to test a number of unanswered questions in the field. Although the mechanism by which tumor cells secrete active AMF in unknown, it has recently been shown that heregulin increases AMF expression by breast cancer cells (49), further supporting an important role for AMF in tumor metastasis in vivo. Since there is no evidence for a normal physiological function or requirement for ligand binding to the AMF receptor in the adult, this receptor:ligand interaction could provide a new, specific target for pharmacological intervention to inhibit tumor metastasis by breast cancer cells to bone and possibly other sites.

REFERENCES (supplemental to those in the original application)

49. AH Talukder, L Adam, A Raz, R Kumar (2000). Heregulin regulation of autocrine motility factor expression in human tumor cells. *Cancer Res* **60**: 4740480.

50. K Shimizu, M Tani, H Watanabe, Y Nagamachi, Y Niinaka, T Shiroishi, S Ohwada, A Raz, J Yokota (1999). The autocrine motility factor receptor gene encodes a novel type of seven transmembrane protein. *FEBS Lett 456*: 295-300.

51. Y-J Sun, C-C Chou, W-S Chen, R-T Wu, M Meng, C-D Hsiao (1999). The crystal structure of a multifunctional protein: Phosphoglucose isomerase/autocrine motility factor/neuroleukin. *Proc Natl Acad Sci USA* **96**: 5412-5417.

52. C-C Chou, Y-J Sun, M Meng, C-D Hsiao (2000). The crystal structure of phosphoglucose isomerase/autocrine motility factor/neuroleukin complexed with its carbohydrate phosphate inhibitors suggests its substrate/receptor recognition. *J Biol Chem*

53. X li, JM Chirgwin (2000). Rabbit phosphoglucose isomerase/neuroleukin/autocrine motility factor: cloning via interspecies identity. *Biochim Biophys Acta* **1476**: 363-367.

54. CJ Jeffery, BJ Bahnson, W Chien, D Ringe, GA Petsko. Crystal structure of rabbit phosphoglucose isomerase, a glycolytic enzyme that moonlights as neuroleukin, autocrine motility factor, and differentiation mediator. *Biochemistry* **39**: 955-964.

55) JJ Yin, K Selander, JM Chirgwin, M Dallas, BG Grubbs, R Wieser, J Massagué, GR Mundy, TA Guise (1999). TGF-β signaling blockade inhibits PTHrP secretion by breast cancer cells and bone metastases development. *J Clin Invest* **103**: 197-206.

APPENDIX

Copies of two papers are attached:

53. X li, JM Chirgwin (2000). Rabbit phosphoglucose isomerase/neuroleukin/autocrine motility factor: cloning via interspecies identity. *Biochim Biophys Acta* **1476**: 363-367.

55) JJ Yin, K Selander, JM Chirgwin, M Dallas, BG Grubbs, R Wieser, J Massagué, GR Mundy, TA Guise (1999). TGF-β signaling blockade inhibits PTHrP secretion by breast cancer cells and bone metastases development. *J Clin Invest* **103**: 197-206.

ELSEVIER

Biochimica et Biophysica Acta 1476 (2000) 363–367

BIOCHIMICA ET BIOPHYSICA ACTA
BBA

www.elsevier.com/locate/bba

Short sequence-paper

Rabbit phosphoglucose isomerase/neuroleukin/autocrine motility factor: cloning via interspecies identity[1]

Xiaochun Li, John M. Chirgwin *

Department of Medicine, Division of Endocrinology and Metabolism, University of Texas Health Science Center, and Veterans Administration Research Service, 7703 Floyd Curl Drive, San Antonio, TX 78284-7877, USA

Received 11 November 1999; received in revised form 7 December 1999; accepted 14 December 1999

Abstract

Phosphoglucose isomerase is the first committed enzyme of glycolysis. The protein also has a variety of biological activities on mammalian cells. The molecular basis of these extracellular functions is unclear, and the high resolution three-dimensional structure of a mammalian enzyme has not been described. We report here the cDNA and protein sequence for phosphoglucose isomerase from rabbit muscle. The sequence was obtained directly by PCR without the need to screen clones from a cDNA library and encoded active enzyme when expressed in bacterial cells. The 558 amino acid rabbit coding sequence is the same length as and highly similar (92% residue identity) to the sequences from human and pig and less so (88%) to the mouse enzyme. Non-conservative amino acid changes between the four mammalian sequences are concentrated in the first 35 and last five residues. The rabbit protein has an additional Cys residue and amino acid changes at five positions otherwise invariant in the mammalian enzymes.

Keywords: Phosphoglucose isomerase; Autocrine motility factor; Neuroleukin

The glycolytic enzyme phosphoglucose isomerase has several alternative names and a variety of biological actions, including effects on peripheral neurons (neuroleukin [1]), tumor cell motility (autocrine motility factor [2]), monocyte differentiation [3], and bone marrow stromal cells (Li and Chirgwin, in preparation). These extracellular activities may be mediated by binding to a recently described receptor [4]. Phosphoglucose isomerase is a 125 kDa homodimer in mammals. The relation of isomerase enzymatic activity to the extracellular biological roles of the protein is not yet clear, although enzymatic activity in the serum of cancer patients has been studied for over 45 years [5] as a marker of metastatic disease.

The crystal structure of a prokaryotic phosphoglucose isomerase from *Bacillus stearothermophilus* was recently published [6]. Although work was begun over 25 years ago to solve the structure of a mammalian enzyme [7,8], high resolution data have not yet been published, in the case of the rabbit protein [9] due to lack of the amino acid sequence. Phosphoglucose isomerase from rabbit skeletal muscle has been commercially available from Sigma for decades, but its sequence has not been described. The rabbit protein has been used extensively because of the similarity of its behavior to the human protein. We therefore undertook to obtain the sequence of phos-

* Corresponding author. Fax: +1-210-567-6693; E-mail: chirgwin@uthscsa.edu

[1] This paper is dedicated to the memory of Professor Ernst A. Noltmann, who pioneered the study of rabbit phosphoglucose isomerase.

0167-4838/00/$ – see front matter
PII: S0167-4838(99)00258-7

phoglucose isomerase from rabbit muscle. The cDNA sequences of human, mouse, and pig proteins were used to design PCR primers to regions conserved between species. Pools of clones from a rabbit cDNA library were amplified with primers for N- and C-terminal regions of the protein. Amplified products were sequenced and used to design a second pair of primers encompassing the complete open reading frame, which was in turn sequenced and then expressed in *Escherichia coli*, where it encoded abundant phosphoglucose isomerase enzymatic activity.

A cDNA library prepared from skeletal muscle of New Zealand white rabbits in λ Zap II vector (2 million primary plaques) was obtained from Stratagene Inc. (cat. 936901). A small aliquot was titered on XLIB MRF′ cells and directly converted into ampicillin-resistant plasmids by a mass excision protocol provided by the manufacturer, using SOLR cells and ExAssist helper phage. The resultant cDNA library, now in pBluescript plasmid, was plated to give 10^4 colonies per 100 mm dish. After 18 h at 37°C, colonies were scraped from 36 plates into 5 ml each of saline, collected by centrifugation, transferred to microfuge tubes, and DNA was individually isolated with a plasmid miniprep kit (Promega) according to the manufacturer's instructions.

Published sequences of mouse (GenBank accession number M14220), human (K03515), and pig (X07382) phosphoglucose isomerase/neuroleukins were aligned with MacVector 6.5 software (Oxford Molecular) to identify regions of extended nucleotide sequence identity. All three cDNAs are about 2 kb with short 5′ untranslated and 1674 base coding sequences. One primer was RPG5c: 5′-GGAATTCAGTCACCATGAGGGGTCCCAGGTC, which includes a 27 base sequence that is identical in all three species, ending at base 522 in human, extending toward the N-terminus, and adding an *Eco*RI site. RPG3: 5′-GGAATTCGCCATGTATGAGCACAAGATC includes a 23 base sequence identical in all three species, extending 3′ from base 1486 in human, and adding an *Eco*RI site.

The cDNAs were non-directional subclones with *Eco*RI adapters in the polylinker of the pBluescript plasmid vector, which provides flanking sites for T3 and T7 primers. Individual pools of the library (50 ng of template DNA) were amplified with a specific primer plus either T3 or T7 primer, using a Taq DNA polymerase kit (Life Technologies) for 25 cycles under standard conditions in an MJ Research minicycler. All pools tested (12) gave a band of the expected size with RPG3-primed reactions. Several pools gave a band of the predicted size with the RPG5-primed reactions. Bands from two independent pools from each primer amplification were purified with a gel extraction kit (Qiagen), digested with *Eco*RI, and ligated into pBluescript which had been digested with *Eco*RI plus alkaline phosphatase. White colonies were selected from X-gal indicator plates and DNAs isolated. These were sequenced using the T3 and T7 primer sites in the vector. RPG5-primed clones (2) gave 45 bases of 5′ut and the first 125 codons of phosphoglucose isomerase, while the RPG3-derived clones (2) gave the last 59 codons of the enzyme followed by 315 nucleotides of 3′ut. One of the clones had an additional five nucleotides of 3′ut (shown in Fig. 1) and an 18 nucleotide polyA tail. Potential polyA addition signals are at positions 1986 (ATAGA, conserved in all four mammalian cDNA sequences) and 1994 (ATAAA, occurring only in the rabbit and pig cDNAs).

A second set of primers was designed from the initial sequence to amplify the entire open reading frame as a 1.7 kb *Hin*dIII to *Eco*RI fragment: RPG-N 5′-CCCAAGCTTCATATGGCCGCGCTCACCCGCAACCCG and RPG-C 5′-CGGAATTCTTAATGGTGATGGTGATGGTGTTGGATTTTGGCCTCACGCTGCTG. The primers convert the bases before the start codon into a unique *Nde*I site and replace the normal stop codon with an extension of six histidine codons followed by a new UAA stop codon. The primers were designed so the DNA could be sequenced as a *Hin*dIII to *Eco*RI insert in pBluescript and also subcloned as an *Nde*I to *Eco*RI insert into the bacterial protein expression vector pET5a. Since the PCR primers were dictated by the template sequence, they were not optimized and required the use of hot-start Taq DNA polymerase for efficient amplification of the target sequence, which was subcloned as before. One of the sequenced pBluescript subclones was digested with *Nde*I and *Hin*dIII to release the coding insert, which was gel purified and ligated into correspondingly double-digested pET5a DNA (Stratagene). The recombinant plasmid was transformed into *E. coli* strain XL1B,

```
                    30                  60                  90                 120
CAGCCGCGGCGCACG TCCCGGTCCGTGCAC CCTGCTGGCCGCGCC ATGGCCGCGCTCACC CGCAACCCGCAGTTC CAGAAGCTGCAGCAA TGGCACCGCGAGCAC GGCTCCGAGCTCAAC
                                 MetAlaAlaLeuThr ArgAsnProGlnPhe GlnLysLeuGlnGln TrpHisArgGluHis GlySerGluLeuAsn> 25

                    150                 180                 210                 240
CTGCGGCACCTTTTC GATACCGACAAGGAG CGCTTCAACCACTTC AGCTTGACGCTCAAC ACCAACCATGGCCAT ATTCTGTTGGATTAC TCCAAGAACCTGGTG ACGGAGGAGGTGATG
LeuArgHisLeuPhe AspThrAspLysGlu ArgPheAsnHisPhe SerLeuThrLeuAsn ThrAsnHisGlyHis IleLeuLeuAspTyr SerLysAsnLeuVal ThrGluGluValMet> 65

                    270                 300                 330                 360
CACATGCTGCTGGAC CTGGCCAAGTCCAGG GGTGTGGAGGCCGCG CGGGAGTCCATGTTC AATGGTGAGAAGATC AACAGCACAGAGGAC CGGGCAGTCCTGCAT GTGGCCCTGCGGAAC
HisMetLeuLeuAsp LeuAlaLysSerArg GlyValGluAlaAla ArgGluSerMetPhe AsnGlyGluLysIle AsnSerThrGluAsp ArgAlaValLeuHis ValAlaLeuArgAsn> 105

                    390                 420                 450                 480
CGCTCCAACACACTC ATTGTGGTGGACGGC AAGGACGTGATGCCG GAAGTCAACAAGGTT CTGGACAAGATGAAG GCCTTCTGCCAGCGG GTCCGCAGTGGCGAC TGGAAGGGGTACACG
ArgSerAsnThrLeu IleValValAspGly LysAspValMetPro GluValAsnLysVal LeuAspLysMetLys AlaPheCysGlnArg ValArgSerGlyAsp TrpLysGlyTyrThr> 145

                    510                 540                 570                 600
GGCAAGACCATCACG GACGTCATCAACATT GGCATCGGTGGCTCC GACCTGGGACCCCTC ATGGTGACCGAAGCT CTGAAGCCATACTCG TCGGGAGGCCCCCGC GTCTGGTTTGTCTCC
GlyLysThrIleThr AspValIleAsnIle GlyIleGlyGlySer AspLeuGlyProLeu MetValThrGluAla LeuLysProTyrSer SerGlyGlyProArg ValTrpPheValSer> 185

                    630                 660                 690                 720
AACATCGATGGGACC CACATTGCCAAAACG CTGGCCTGCCTGAAC CCCGAGTCGTCCCTG TTCATCATCGCCTCC AAGACCTTTACCACC CAGGAGACCATCACG AACGCAGAGACGGCC
AsnIleAspGlyThr HisIleAlaLysThr LeuAlaCysLeuAsn ProGluSerSerLeu PheIleIleAlaSer LysThrPheThrThr GlnGluThrIleThr AsnAlaGluThrAla> 225

                    750                 780                 810                 840
AAGGACTGGTTTCTC CTGTCCGCCAAGGAT CCTTCTACAGTTGCG AAACACTTTGTCGCG CTGTCTACTAACACG GCCAAAGTGAAAGAG TTTGGAATTGACCCT CAAAACATGTTCGAG
LysAspTrpPheLeu LeuSerAlaLysAsp ProSerThrValAla LysHisPheValAla LeuSerThrAsnThr AlaLysValLysGlu PheGlyIleAspPro GlnAsnMetPheGlu> 265

                    870                 900                 930                 960
TTCTGGGACTGGGTG GGAGGACGCTACTCG CTGTGGTCAGCCATC GGCCTCTCCGTCGCC CTGCACGTGGGTTTT GACAACTTCGAGCAG CTGCTCTCCGGGGCT CACTGGATGGACCAG
PheTrpAspTrpVal GlyGlyArgTyrSer LeuTrpSerAlaIle GlyLeuSerValAla LeuHisValGlyPhe AspAsnPheGluGln LeuLeuSerGlyAla HisTrpMetAspGln> 305

                    990                 1020                1050                1080
CACTTCCGCACGACG CCCCTGGAGAAGAAC GCCCCCGTCCTGCTG GCCATGCTGGGGATC TGGTACATCAACTGC TTTGGGTGTGAGACT CAGGCCGTGCTGCCC TATGACCAGTACCTG
HisPheArgThrThr ProLeuGluLysAsn AlaProValLeuLeu AlaMetLeuGlyIle TrpTyrIleAsnCys PheGlyCysGluThr GlnAlaValLeuPro TyrAspGlnTyrLeu> 345

                    1110                1140                1170                1200
CACCGCTTTGCAGCC TACTTCCAGCAGGGT GACATGGAGTCCAAT GGGAAGTACATCACC AAGTCCGGCGCCCGT GTGGACCACCAGACG GGCCCCATTGTGTGG GGGGAGCCGGGGACC
HisArgPheAlaAla TyrPheGlnGlnGly AspMetGluSerAsn GlyLysTyrIleThr LysSerGlyAlaArg ValAspHisGlnThr GlyProIleValTrp GlyGluProGlyThr> 385

                    1230                1260                1290                1320
AACGGCCAGCATGCC TTCTACCAGCTCATC CACCAAGGCACCAAG ATGATACCCTGTGAC TTCCTCATCCCAGTC CAGACCCAGCACCCG ATCCGGAAGGGTCTG CACCACAAGATCCTG
AsnGlyGlnHisAla PheTyrGlnLeuIle HisGlnGlyThrLys MetIleProCysAsp PheLeuIleProVal GlnThrGlnHisPro IleArgLysGlyLeu HisHisLysIleLeu> 425

                    1350                1380                1410                1440
CTGGCCAACTTTCTA GCGCAGACCGAGGCC CTGATGAAGGGGAAA TCGACAGAGGAGGCC CGTAAGGAGCTGCAG GCTGCAGGCAAGAGT CCCGAGGACCTCATG AAGCTGCTGCCACAC
LeuAlaAsnPheLeu AlaGlnThrGluAla LeuMetLysGlyLys SerThrGluGluAla ArgLysGluLeuGln AlaAlaGlyLysSer ProGluAspLeuMet LysLeuLeuProHis> 465

                    1470                1500                1530                1560
AAGGTCTTTGAAGGA AATCGCCCAACGAAC TCTATCGTGTTCACG AAGCTCACACCATTC ATCCTTGGAGCCTTG ATCGCCATGTATGAG CACAAGATCTTCGTC CAGGGCGTCGTCTGG
LysValPheGluGly AsnArgProThrAsn SerIleValPheThr LysLeuThrProPhe IleLeuGlyAlaLeu IleAlaMetTyrGlu HisLysIlePheVal GlnGlyValValTrp> 505

                    1590                1620                1650                1680
GACATCAACAGCTTC GACCAGTGGGGAGTG GAGTTGGGAAAGCAG CTGGCTAAGAAGATC GAGCCGGAGCTGGAC GGCAGCAGTCCCGTG ACCTCTCACGACTCC TCCACCAACGGGCTC
AspIleAsnSerPhe AspGlnTrpGlyVal GluLeuGlyLysGln LeuAlaLysLysIle GluProGluLeuAsp GlySerSerProVal ThrSerHisAspSer SerThrAsnGlyLeu> 545

                    1710                1740                1770                1800
ATCAACTTCATCAAG CAGCAGCGTGAGGCC AAAATCCAATAAACT CGTGTTCGGCCGCAA CCCCTGTCGTGACTG GTCCTTGTCCCACCT CACCAGAGTCTGCAC TGCATGGCCCTGGCC
IleAsnPheIleLys GlnGlnArgGluAla LysIleGln***>

                    1830                1860                1890                1920
CTCCCTGCCCAGAGC ACTCTCGGGCCGTGG GCTTAGACCCCCAGC CCCTTGAGTGGGTGG GGTGGGGCACTCGAA GCCAGTCTGGATCCA CCACTGCCACCCCTT CGACGTCCACTGTCC

                    1950                1980                2010
CTGTTTTACGATTGG CTGAAGTGTGTCAGT GCCGCTGATTCGTTT GACCTGTGATCACAT CTCAAATAGAAAAAT AAAGATGTCACAAAG G
```

Fig. 1. Sequence of 2011 nucleotide rabbit phosphoglucose isomerase cDNA and the 558 amino acid open reading frame. Spaces are at 15 base/5 amino acid intervals. DNA numbering is above the sequence and protein numbering at the right margin.

purified, and verified by restriction mapping. It was then transferred into the specialized host cells BL21DE3pLysS (Stratagene). Protein expression was induced according to standard conditions [10] with 0.3 mM isopropylthiogalactoside, and the cells were harvested after 3 h at 30°C. Cell cytosols were isolated by sonication and centrifugation. The soluble supernatants were assayed for phosphoglucose isomerase enzymatic activity by monitoring the conversion of fructose 6-phosphate to glucose 6-phosphate using a standard coupled spectrophotometric assay [11]. Protein concentrations were determined with a commercial dye binding kit (Pierce). Oligonucleotide synthesis and DNA sequencing (fully con-

firmed on both strains) were carried out by the Center for Advanced DNA Technologies, Department of Microbiology.

Fig. 1 shows the composite complete cDNA sequence for phosphoglucose isomerase from skeletal muscle of New Zealand white rabbit. Except for the last five bases of the 3′ untranslated sequence and the polyA tail, identical sequences were obtained from clones isolated from separate pools of the library. The untranslated regions are of similar extent to those reported for the cDNAs from mouse, human, and pig. The 558 amino acid protein sequence is entirely co-linear with those from the other species and shows substantial amino acid sequence identity to human (92%), pig (92%), and mouse (88%) enzymes. The sequence is available from GenBank: accession number AF199601. The subunit molecular weight (62 744, and pI = 7.25 were calculated with the MacVector Protein Toolbox) shows good agreement and the amino acid composition excellent agreement with the values experimentally determined 30 years ago by classical means [12]. The mammalian enzymes have four conserved cysteine residues (with Cys330 changed to Phe in the pig). The rabbit enzyme has a fifth cysteine at non-conserved position 198. It also has five amino acid changes at otherwise invariant positions: Ser131Ala, Ala238Thr, Leu322Met, Asn329Ser, and Glu460Met. (The residue before the number is found in mouse, pig, and human; the residue after the number is found in rabbit.) All the mammalian enzymes show highly conserved core sequences. Variable residues are concentrated at the N-terminus (eight variable positions between residues 15 and 35) and the C-terminus (last five residues). The significance of these sequence variations should become clear when high resolution structures of rabbit and pig enzymes are published.

Sequence alignment shows no gaps in the 558 amino acid coding sequences of the four mammalian cDNAs. The bacterial enzymes are over 100 amino acids shorter, with many deletions [6]. Surprisingly, substantial blocks of conserved nucleotide sequence also occur throughout the mammalian 3′ untranslated regions, along with gaps and insertions. Untranslated regions seldom show interspecies conservation. The data suggest that the 3′ut of phosphoglucose isomerase could serve a regulatory or other function. Both at the DNA and protein

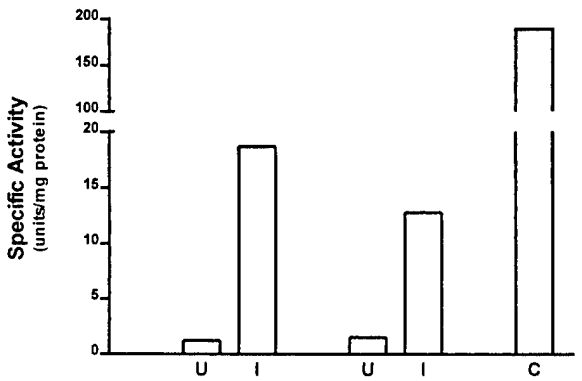

Fig. 2. Bacterial expression of rabbit phosphoglucose isomerase enzymatic activity. *E. coli* cells carrying two independently derived clones of the C-terminally $(His)_6$-extended rabbit DNA in the pET5a vector were grown to $A_{600\,nm} = 0.5$ and induced for 3 h. Cell lysates were cleared by centrifugation and equivalent amounts assayed. Results were expressed as specific activity of induced (I) versus uninduced (U) samples and compared to that of commercial (C) rabbit enzyme (Sigma).

levels, human and pig sequences show the highest identity, while the rabbit is slightly more distant from these two. The mouse sequence is considerably more diverged. These sequence relationships are consistent with our observation that the effects of mouse phosphoglucose isomerase are specific for mouse bone marrow cells, while rabbit and human proteins are both active on human marrow cells (Li et al., in preparation).

Fig. 2 demonstrates phosphoglucose isomerase catalytic activity directed by the cloned sequence, compared to the empty vector control. The activity of the rabbit enzyme is similar to that obtained with the mouse and human proteins when expressed with C-terminal $(His)_6$ tags, and all can be purified to homogeneity by metal chelate affinity chromatography (Li et al., in preparation). Induction of the bacterial cultures resulted in an approximately 10-fold increase in isomerase activity. The specific activity of the induced lysate was 10% that of the highly purified commercial enzyme. The C-terminal $(His)_6$ tag will facilitate future purification of the enzyme with site-directed mutations which may interfere with activity.

The elucidation of the rabbit muscle phosphoglucose isomerase sequence required only four custom PCR primers and a commercially available rabbit cDNA library. No screening of the library as plaques or colonies was required. The inducible activity when

expressed in the pET5a vector confirmed that the coding information was correct; it also provides a substantial source of the recombinant rabbit enzyme, which can be purified by standard Ni-NTA agarose affinity chromatography (not shown). The public databases contain many sequences in the form of ESTs from mouse and man. However, few sequence data for species such as rabbit are available. We used the published sequences of phosphoglucose isomerase/neuroleukin from mouse, human, and pig to design primers to amplify the 2 kb full-length sequence of the homologous cDNA from rabbit. The strategy was PCR based and required very little commitment of labor or resources. This approach could be applied to the rapid isolation and expression of protein sequences of interest from organisms which are not yet the subject of extensive sequence analysis.

The availability of the rabbit protein sequence should facilitate interpretation of the rabbit crystallographic data [9]. A three-dimensional structure of a mammalian protein will permit analysis of the relation between intracellular isomerase activity and the extracellular biological activities, as well as comparison of the structures of mammalian and bacterial isomerases [6] and assessing the controversial claim that the enzyme from *B. stearothermophilus* has activity in the mammalian factor bioassays.

This research was supported by a grant from the U.S. Army Breast Cancer Research Program and a Merit Award from the Veterans Administration Research Service to J.M.C.

References

[1] M.E. Gurney, S.P. Heinrich, M.R. Lee, H.-S. Yu, Molecular cloning and expression of neuroleukin, a neurotrophic factor for spinal and sensory neurons, Science 234 (1986) 566–574.

[2] H. Watanabe, K. Takehana, M. Date, T. Shinozaki, A. Raz, Tumor cell autocrine motility factor is the neuroleukin/phosphohexose isomerase polypeptide, Cancer Res. 56 (1996) 2960–2963.

[3] W. Xu, K. Seiter, E. Feldman, T. Ahmed, J.W. Chiao, The differentiation and maturation mediator for human myeloid leukemia cells shares homology with neuroleukin or phosphoglucose isomerase, Blood 87 (1996) 4502–4506.

[4] K. Shimizu, M. Tani, H. Watanabe, Y. Nagamachi, Y. Niinaka, T. Shiroishi, S. Ohwada, A. Raz, J. Yokata, The autocrine motility factor receptor gene encodes a novel type of seven transmembrane protein, FEBS Lett. 456 (1999) 295–300.

[5] O. Bodansky, Serum phosphohexose isomerase in cancer II. As an index of tumor growth in metastatic cancer of the breast, Cancer 7 (1954) 1200–1226.

[6] Y.-J. Sun, C.-C. Chou, W.-S. Chen, R.-T. Wu, M. Meng, C.-D. Hsiao, The crystal structure of a multifunctional protein: phosphoglucose isomerase/autocrine motility factor/neuroleukin, Proc. Natl. Acad. Sci. USA 96 (1999) 5412–5417.

[7] H. Muirhead, P.J. Shaw, Three-dimensional structure of pig muscle phosphoglucose isomerase at 6 Å resolution, J. Mol. Biol. 89 (1974) 195–203.

[8] A. Achari, S.E. Marshall, H. Muirhead, R.H. Palmieri, E.A. Noltmann, Glucose-6-phosphate isomerase, Phil. Trans. R. Soc. Lond. B 293 (1981) 145–157.

[9] W. Kugler, K. Breme, P. Laspe, H. Muirhead, C. Davies, H. Winkler, Molecular basis of neurological dysfunction coupled with hemolytic anemia in human glucose-6-phosphate isomerase (GPI) deficiency, Hum. Genet. 103 (1998) 450–454.

[10] F.W. Studier, B.A. Moffatt, Use of bacteriophage T7 RNA polymerase to direct selective high-level expression of cloned genes, J. Mol. Biol. 189 (1986) 113–130.

[11] E.A. Noltmann, Phosphoglucose isomerase I. Rabbit muscle (crystalline), Methods Enzymol. 9 (1966) 557–565.

[12] N.G. Pon, K.D. Schnackerz, M.N. Blackburn, G.C. Chatterjee, E.A. Noltmann, Molecular weight and amino acid composition of five-times-crystallized phosphoglucose isomerase from rabbit skeletal muscle, Biochemistry 9 (1970) 1506–1514.

TGF-β signaling blockade inhibits PTHrP secretion by breast cancer cells and bone metastases development

Juan Juan Yin,[1] Katri Selander,[1] John M. Chirgwin,[1] Mark Dallas,[1] Barry G. Grubbs,[1] Rotraud Wieser,[2] Joan Massagué,[2] Gregory R. Mundy,[1] and Theresa A. Guise[1]

[1]Department of Medicine, University of Texas Health Science Center at San Antonio, San Antonio, Texas 78284-7877, USA
[2]Howard Hughes Medical Institute, Memorial Sloan-Kettering Cancer Center, New York, New York, 10021 USA

Address correspondence to: T.A. Guise, Division of Endocrinology, Department of Medicine, University of Texas Health Science Center at San Antonio, 7703 Floyd Curl Drive, San Antonio, Texas 78284-7877, USA. Phone: (210) 567-4900; Fax: (210) 567-6693; E-mail: guise@uthscsa.edu

Juan Juan Yin and Katri Selander contributed equally to this work.

Received for publication March 25, 1998, and accepted in revised form December 1, 1998.

Breast cancer frequently metastasizes to the skeleton, and the associated bone destruction is mediated by the osteoclast. Growth factors, including transforming growth factor-β (TGF-β), released from bone matrix by the action of osteoclasts, may foster metastatic growth. Because TGF-β inhibits growth of epithelial cells, and carcinoma cells are often defective in TGF-β responses, any role of TGF-β in metastasis is likely to be mediated by effects on the surrounding normal tissue. However, we present evidence that TGF-β promotes breast cancer metastasis by acting directly on the tumor cells. Expression of a dominant-negative mutant (TβRIIΔcyt) of the TGF-β type II receptor rendered the human breast cancer cell line MDA-MB-231 unresponsive to TGF-β. In a murine model of bone metastases, expression of TβRIIΔcyt by MDA-MB-231 resulted in less bone destruction, less tumor with fewer associated osteoclasts, and prolonged survival compared with controls. Reversal of the dominant-negative signaling blockade by expression of a constitutively active TGF-β type I receptor in the breast cancer cells increased tumor production of parathyroid hormone-related protein (PTHrP), enhanced osteolytic bone metastasis, and decreased survival. Transfection of MDA-MB-231 cells that expressed the dominant-negative TβRIIΔ-cyt with the cDNA for PTHrP resulted in constitutive tumor PTHrP production and accelerated bone metastases. These data demonstrate an important role for TGF-β in the development of breast cancer metastasis to bone, via the TGF-β receptor-mediated signaling pathway in tumor cells, and suggest that the bone destruction is mediated by PTHrP.

J. Clin. Invest. **103**:197–206 (1999).

Introduction

In 1889, Paget (1) proposed the "seed and soil" hypothesis to explain the predilection with which breast cancer grows in bone. Despite these observations, the mechanisms underlying the affinity with which breast cancer grows in bone are not completely understood. Breast cancer metastasizes to bone in greater than 80% of patients with advanced disease and causes local osteolysis (2). The associated pain, pathological fracture, hypercalcemia, and nerve compression syndromes are consequences of the bone destruction. These morbid complications can be devastating, because patients with breast cancer and bone metastases may survive for many years.

A unique characteristic of the skeleton is the storage within bone matrix of immobilized growth factors such as transforming growth factor (TGF)-β, insulin-like growth factor (IGF)-1 and -2, fibroblast growth factor (FGF)-1 and -2, and platelet-derived growth factors (3). The most abundant repository for TGF-β is the bone matrix, and it is released locally in the microenvironment as a consequence of osteoclastic bone resorption (4). Thus, tumor cells with the capacity to stimulate osteoclastic bone resorption may enrich the bone microenvironment with growth factors that may alter behavior of tumor cells. Data in support of this include histological examination of breast cancer metastatic to bone, which reveals tumor cells adjacent to bone-resorbing osteoclasts (5). Bisphosphonates, potent inhibitors of osteoclastic bone resorption, decrease the morbidity associated with breast cancer bone metastases (6, 7). These findings indicate that the bone destruction by breast cancer is mediated by tumor stimulation of osteoclastic bone resorption.

Parathyroid hormone-related protein (PTHrP) is a tumor product (8–10) that stimulates osteoclastic bone resorption and renal tubular reabsorption of calcium by binding to a common PTH/PTHrP receptor (11, 12). The majority of patients with solid tumors and hypercalcemia have increased plasma PTHrP concentrations (13). PTHrP may have a more common role in malignancy as a mediator of osteolytic bone metastasis in breast cancer, even in the absence of hypercalcemia. Women with PTHrP-positive primary breast tumors are more likely to develop bone metastases (14). Human breast cancer cells express PTHrP more often in bone (15) than in the primary (16) or soft tissue sites, and neutralizing antibodies to PTHrP inhibit the development of osteolytic metastases by human breast cancer cells *in vivo* (17). The reasons for increased expression of PTHrP in bone are unknown, but bone-derived growth factors may be responsible.

Because TGF-β is one of the most abundant growth

factors in bone matrix (3), is released in active form during osteoclastic bone resorption (4), and increases PTHrP expression by cancer cells *in vitro* (18–21), we postulated that TGF-β was responsible for enhancing PTHrP production in the bone microenvironment and the subsequent bone destruction. To test this hypothesis, the human breast cancer cell line MDA-MB-231 (22) was transfected with a cDNA encoding a TGF-β type II receptor lacking most of the cytoplasmic domain (TβRIIΔcyt), which acts as a dominant-negative to block the biologic effects of TGF-β (23). Expression of this mutant receptor in human breast cancer cells inhibited TGF-β–stimulated PTHrP production and blocked the growth inhibitory effects of TGF-β *in vitro*. Blockade of TGF-β responsiveness in breast cancer cells resulted in decreased osteolysis, less tumor burden in bone, and enhanced survival in mice bearing tumors that expressed the dominant-negative receptor. When TGF-β responsiveness of the breast cancer cells expressing the dominant-negative type II receptor was restored by expression of a constitutively active TGF-β type I receptor subunit, growth of tumor in bone and osteolysis were markedly enhanced, and survival was decreased. Because PTHrP production was increased fivefold in this tumor line, the data suggested that the effects of TGF-β to enhance bone destruction were mediated by PTHrP. To confirm this notion, a cDNA-encoding human PTHrP was transfected into the breast cancer cells expressing the dominant-negative type II receptor. The resulting increase in constitutive PTHrP production *in vitro* was associated with accelerated bone metastases *in vivo*.

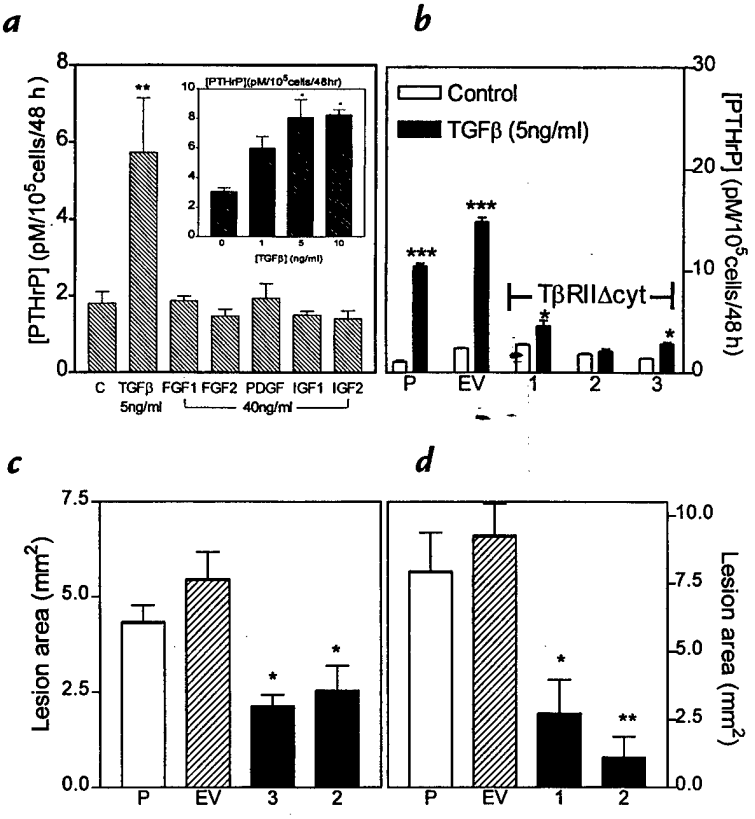

Figure 1

(*a*) Effects of bone growth factors on PTHrP secretion from MDA-MB-231 cells *in vitro*. MDA-MB-231 cells were plated onto 48-well plates and grown to near confluence. Cells were washed and treated with serum-free media containing the respective growth factors for 48 h. PTHrP concentrations in conditioned media were corrected for cell number. Only the results for the highest concentration of each growth factor are shown. *Inset:* Dose response for PTHrP secretion by MDA-MB-231 cells treated with TGF-β. Values represent the mean ± SEM ($n = 3$ per group).(*b*) Effect of TGF-β on PTHrP secretion by MDA-MB-231, MDA/pcDNA3, and MDA/TβRIIΔcyt clones. Respective cells were plated onto 48-well plates and treated as described in *a*. Values represent the mean ± SEM ($n = 3$ per group). *P* = parental MDA-MB-231; *EV* = empty vector pcDNA3 clone; 1, 2, and 3 are respective MDA/TβRIIΔcyt clones. (*c* and *d*) Osteolytic lesion area from radiographs of two separate experiments comparing clones 3 and 2 (*c*) or clones 1 and 2 (*d*) with controls of MDA-MB-231 (*P*) or pcDNA3 vector (*EV*). Values represent mean ± SEM ($n = 4$ per group). $^*P < 0.05$, $^{**}P < 0.01$, $^{***}P < 0.001$ vs. controls. *PTHrP*, parathyroid hormone-related protein; *TGF-β*, transforming growth factor-β.

Methods

Cells. MDA-MB-231 cells were cultured in DMEM (Life Technologies Inc., Rockville, Maryland, USA) containing 10% FCS (HyClone Laboratories, Logan, Utah, USA), 1% penicillin/streptomycin, and nonessential amino acids (GIBCO BRL, Gaithersburg, Maryland, USA). To test the effect of bone-derived growth factors on PTHrP secretion by MDA-MB-231 cells, 10^4 cells/ml were plated onto 48-well plates. When near confluence, cells were washed with PBS, and 250 μl of serum-free DMEM containing the following growth factors was added to each well: TGF-β1 (0, 1, 5, or 10 ng/ml), FGF-1 (0, 4, 20, or 40 ng/ml), FGF-2 (0, 4, 20, or 40 ng/ml), PDGF (0, 1, 5, 10, or 40 ng/ml), IGF-1 (0, 1, 5, 10, or 40 ng/ml), and IGF-2 (0, 1, 5, 10, or 40 ng/ml). TGF-β1, FGF-1, FGF-2, PDGF, IGF-1, and IGF-2 were purchased from R&D Systems Inc. (Minneapolis, Minnesota, USA). Conditioned media were collected after 48 h, stored at –70°C for PTHrP measurement, and cell number was counted for each well to correct the PTHrP concentration of the conditioned media. Triplicate measurements were performed for each treatment.

To measure the effects of TGF-β on the growth rate of MDA-MB-231 cells and respective clones, 10^4 cells/ml were plated onto each of two 24-well plates. One plate was treated with TGF-β1 (20 ng/ml) and the other with vehicle. Cell number was counted daily for 8 days; each measurement was performed in triplicate.

Stable transfection of MDA-MB-231 cells with cDNA for the truncated type II TGF-β receptor (TβRIIΔcyt). TβRIIΔcyt cDNA (23) was subcloned from pMEP4 into the pcDNA3 expression vector (Invitrogen Corp., Carlsbad, California, USA) as a *Hin*dIII–*Bam*HI fragment. The pcDNA3/TβRIIcyt DNA or the empty vector, pcDNA3, was transfected into MDA-MB-231 cells by calcium phosphate precipitation. Single clones were isolated by limiting dilution in the presence of the selective marker, G418 (Sigma Chemical Co., St. Louis, Missouri, USA). Clones were screened by measuring the amount of secreted PTHrP in serum-free 48-h conditioned media in the presence or absence of TGF-β (5 ng/ml). Clones in which PTHrP secretion did not increase in response to TGF-β were selected for further study.

Stable transfection of MDA/TβRIIΔcyt with cDNA for the constitutively active type I TGF-β receptor TβRI(T204D). The

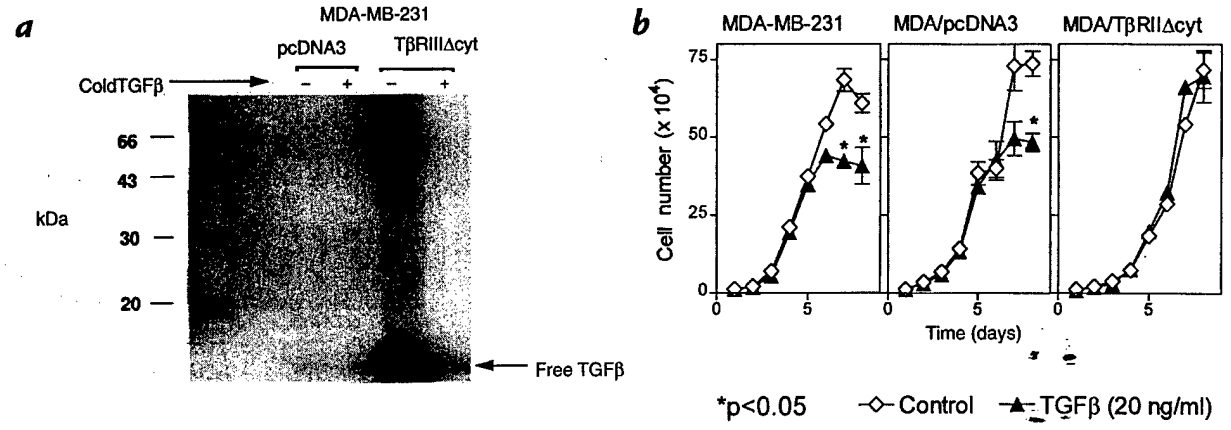

Figure 2

(*a*) ^{125}I-labeled TGF-β1 cross-linking followed by immunoprecipitation with anti-HA antibody in clonal MDA-MB-231 cells expressing the TβRIIΔcyt (*MDA/TβRIIΔcyt*) or the empty vector (*MDA/pcDNA3*). Clonal lines were cross-linked with 160 pM ^{125}I-labeled TGF-β1 alone (-) or in the presence of excess unlabeled TGF-β1 (5 nM) (+). Cell extracts were subjected to SDS-PAGE and autoradiography to visualize the truncated receptor. (*b*) Effect of TGF-β on growth rate of MDA-MB-231, MDA/pcDNA3, and MDA/TβRIIΔcyt cells. Respective cells were plated at a density of 10^4 cells per well with or without TGF-β (20 ng/ml) in 10% FCS and counted daily. Values represent the mean ± SEM (n = 3 per group). In the absence of TGF-β, growth rates of each cell line did not significantly differ.

TβRI(T204D) cDNA insert (24, 25) was subcloned into pcDNA3.1zeo (Invitrogen Corp.) as a *Hin*dIII-*Bam*HI fragment. The pcDNA3.1zeo/TβRI(T204D) DNA or the empty vector, pcDNA3.1zeo, was transfected into the MDA-MB-231 clonal line expressing the truncated type II TGF-β receptor, MDA/TβRIIΔcyt, by calcium phosphate precipitation. Single clones were isolated by limiting dilution in the presence of the selective markers, G418 and zeocin (Invitrogen Corp.), and screened as described. Clones with increased PTHrP production, basally and in response to TGF-β1, were selected for further study.

Stable transfection of MDA/TΔRIIΔcyt with cDNA for PTHrP. Human preproPTHrP cDNA encoding the 1-141 isoform was subcloned from pCMVIE-AK1-DHFR (26) into pcDNA3.1zeo (Invitrogen Corp.) as a *Hin*dIII-*Bam*HI fragment. The pcDNA3.1zeo/PTHrP DNA or the empty vector, pcDNA3.1zeo, was transfected into the MDA-MB-231 clonal line expressing the truncated type II TGF-β receptor, MDA/TβRIIΔcyt, by calcium phosphate precipitation. Single clones were isolated by limiting dilution in the presence of both selective markers, G418 and zeocin (Invitrogen Corp.), and screened as described. Clones with increased PTHrP production, in the basal state, and which did not respond to TGF-β1, were selected for further study.

Cross-linking and immunoprecipitation. MDA-MB-231 clones expressing either TβRIIΔcyt (MDA/TβRIIΔcyt) or the empty vector (MDA/pcDNA3) were plated onto two 10-cm petri dishes (10^6 cells per dish). Cells were grown to confluence and incubated for 3 h at 4°C with ^{125}I-labeled TGF-β1 (160 pM) (Du Pont Nen Research Products, Boston, Massachusetts, USA) alone or with cold TGF-β1 (5 nM) as a competitor (23). After washing away the unbound TGF-β1, ligand-receptor was cross-linked with disuccinimidyl suberate and solubilized with 10 mM Tris buffer (pH 7.4) containing 1% Triton X-100, 1 mM EDTA, and protease inhibitors. The receptor complexes were immunoprecipitated with 2.5 μg/ml mouse anti-HA monoclonal antibody, 12CA5 (Boehringer Mannheim Biochemicals, Indianapolis, Indiana, USA), followed by adsorption to protein G-Sepharose (Pharmacia Biotech Inc., Piscataway, New Jersey, USA). This mixture was washed, and bound protein was eluted by heating samples in SDS-PAGE sample buffer containing 100 mM dithiothreitol. Samples were run on 12.5% SDS-PAGE gels under reducing conditions, and gels were fixed, dried, and exposed to film at -70°C.

Animals

Animal protocols were approved by the Institutional Animal Care and Use Committee at the University of Texas Health Science Center at San Antonio and were in accordance with the National Institutes of Health *Guide for the Care and Use of Laboratory Animals.* Female nude mice 4 weeks of age were housed in laminar flow isolated hoods. Water supplemented with vitamin K and autoclaved mouse chow were provided *ad libitum.* Whole blood samples for ionized calcium concentration were obtained by retro-orbital puncture under metofane anesthesia. Blood for PTHrP measurement was similarly obtained and collected on ice in Vacutainer tubes containing EDTA and 400 IU/ml aprotinin (Sigma Chemical Co.). Tumor inoculation into the left cardiac ventricle was performed as described previously (17).

Experimental protocols

Bone metastasis. In the pilot experiments (Fig. 1, *c* and *d*), mice were inoculated with tumor-cell suspensions of MDA/TβRIIΔ-cyt (independent clones: 1, 2, and 3), MDA/pcDNA3, or parental MDA-MB-231 cells into the left cardiac ventricle (n = 4 per group) on day 0. At sacrifice, on day 28, radiographs were obtained and analyzed as described later in this paper. Because MDA/TβRIIΔcyt, clone 2, was the least responsive to TGF-β *in vitro* (Fig. 1*b*), more detailed experiments were performed comparing this clone with the controls. In the first set of experiments, mice were inoculated with tumor-cell suspensions of MDA/TβRIIΔcyt (clone 2), MDA/pcDNA3, or parental MDA-MB-231 cells into the left cardiac ventricle (n = 13 per group) on day 0 after baseline radiographs, body weights, and blood for Ca^{2+} and plasma PTHrP concentrations were obtained. Radiographs were taken on day 21 and at sacrifice on day 24 to monitor progression of osteolytic metastases. Ca^{2+} and body weight were measured weekly after tumor inoculation until sacrifice, at which time most control mice were cachectic and paraplegic. Blood was collected for Ca^{2+} and PTHrP measurement, and all bones and soft tissues were fixed in formalin for histologic analysis. Autopsy was performed on all mice, and those with tumor in the chest were excluded from analysis, because this indicated that the tumor inoculum did not properly enter the left cardiac ventricle. A separate experiment was similarly performed to assess sur-

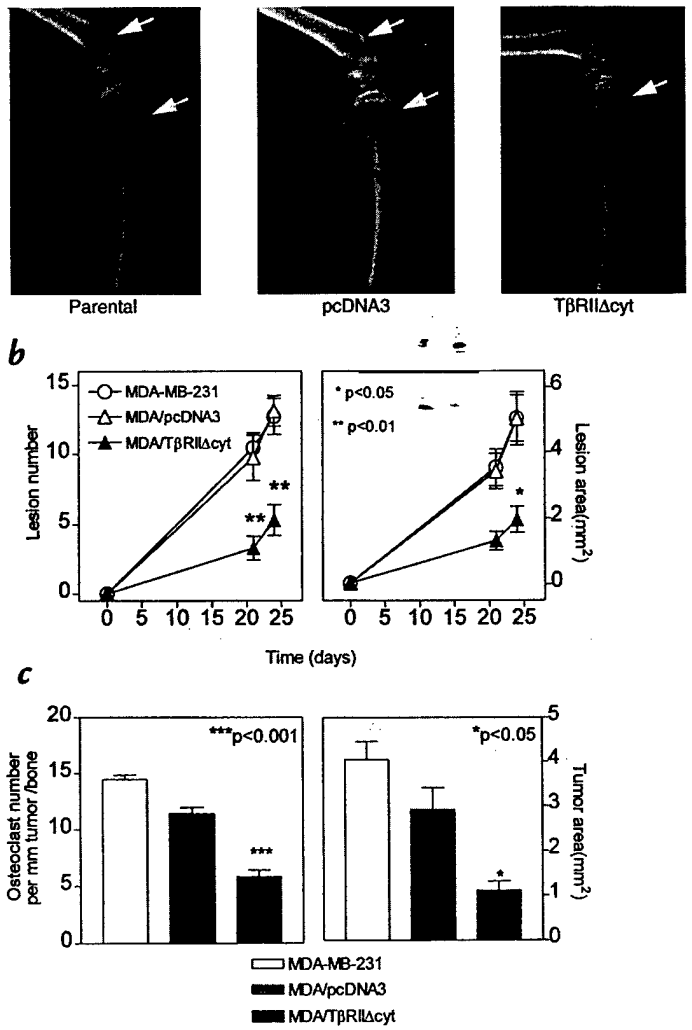

Figure 3
(*a*) Representative radiographs of hindlimbs from mice bearing MDA-MB-231, MDA/pcDNA3, or MDA/TβRIIΔcyt tumors 24 days after tumor inoculation. Osteolytic lesions are indicated by the arrows. (*b*) Osteolytic lesion number and area on radiographs as measured by computerized image analysis of forelimbs and hindlimbs. Respective tumor cells were inoculated on day 0. Values represent the mean ± SEM (n = 13 per group). (*c*) Histomorphometric analysis of forelimbs and hindlimbs from mice with osteolytic lesions. Data represent measurements from midsections of tibiae, femora, and humeri of mice from *b*, inoculated with either MDA-MB-231, MDA/pcDNA3, or MDA/TβRIIΔcyt clone 2. Tumor area (mm^2) from metastatic bone lesions is illustrated on the right and osteoclast number per millimeter of tumor adjacent to bone (tumor/bone interface) on the left. Values represent the mean ± SEM.

vival. In this experiment, mice were sacrificed when they became moribund.

In the second set of experiments, female mice were inoculated with tumor-cell suspensions of clonal MDA-MB-231 lines TβRIIΔcyt + TβRI(T204D) or TβRIIΔcyt + pcDNA3.1zeo into the left cardiac ventricle on day 0. Radiographs, body weight, and blood for Ca^{2+} and PTHrP were obtained at baseline and sacrifice as in the first set of experiments. Ca^{2+}, body weight, and radiographs were monitored weekly for 4 weeks, at which time the mice were sacrificed. Tissue processing, autopsy, data analysis, and a separate survival experiment were performed as in the first experiment.

In the third set of experiments, female mice were inoculated with tumor-cell suspensions of clonal MDA-MB-231 lines TβRIIΔcyt + PTHrP (two different clones) or TβRIΔcyt + pcDNA3.1zeo into the left cardiac ventricle on day 0. The same parameters were measured as in the previous experiments. Two separate experiments were performed using two different TβRIIΔcyt + PTHrP clones. Four TβRIΔcyt + PTHrP clones were studied in total.

Local tumor growth. To investigate whether expression of the dominant-negative type II TGF-β receptor subunit in breast cancer cells altered tumor growth in sites other than bone, tumor-cell suspensions (10^7/100 μl PBS) of either MDA/TβRIIΔcyt, MDA/pcDNA3, or parental MDA-MB-231 cells were inoculated into the right thigh of female nude mice. Tumor volume was measured with calipers and calculated by the formula of an ovoid where L equals midaxis length and W equals midaxis width: tumor volume = $4/3\pi \times L/2\ (W/2)^2$.

Analytical methods

Ca^{2+} measurement. Ca^{2+} concentrations were measured in whole blood using a Ciba Corning 634 ISE Ca^{2+}/pH analyzer (Corning Medical and Scientific Medfield, Massachusetts, USA) as described previously (17).

PTHrP assay. PTHrP concentrations were measured in conditioned media and plasma using a two-site immunoradiometric assay (Nichols Institute, San Juan Capistrano, California, USA) that detects PTHrP-(1–72) and has a calculated sensitivity of 0.3 pmol/l (27). PTHrP concentrations in conditioned media samples were calculated from a standard curve generated by adding recombinant PTHrP-(1–86) to the specific type of medium (unconditioned) used and were considered undetectable if media concentrations were <0.3 pmol/l before correction for cell number.

Radiographs and measurement of osteolytic lesion area. Animals were x-rayed in a prone position against the film as described previously (17). All radiographs were evaluated without knowledge of treatment groups. The area of osteolytic bone metastases was calculated using a computerized image analysis system. Video images of radiographs were captured using a frame grabber board on a PC system. Quantitation of lesion area was performed using image analysis software (Java, Jandal Video analysis; Jandel Scientific, Corte Madera, California, USA).

Bone histology and histomorphometry. Forelimb and hindlimb bones were removed from mice at time of killing, fixed in 10% buffered formalin, decalcified in 14% EDTA, and embedded in paraffin wax. Sections were stained with hematoxylin, eosin, orange G, and phloxine. The following variables were measured in midsections of tibiae and femora, without knowledge of experimental groups, to assess tumor involvement: total tumor area and osteoclast number per millimeter of tumor/bone interface. Histomorphometric analysis was performed on an OsteoMeasure System (Osteometrics Inc., Atlanta, Georgia, USA).

Statistical analysis

Results are expressed as the mean ± SEM. Data were analyzed by analysis of variance followed by Tukey-Kramer post test. Log-rank test (Wilcox survival) was used to analyze survival data. $P < 0.05$ was considered significant.

Results

Effects of bone growth factors on PTHrP production in vitro by MDA-MB-231 cells. Because previous clinical and experimental studies demonstrated increased PTHrP expression by breast cancer cells in the bone microenviron-

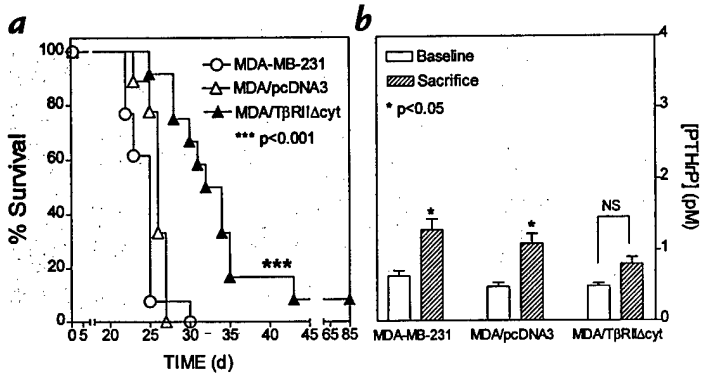

Figure 4
Survival (*a*) and plasma PTHrP concentrations (*b*) in mice bearing MDA-MB-231, MDA/pcDNA3, or MDA/TβRIIΔ–cyt tumors. (*a*) Survival of mice bearing MDA/TΔRIIΔcyt tumors was significantly longer than that of the controls. (*b*) Plasma PTHrP concentrations at sacrifice were significantly higher than respective concentrations before tumor inoculation (baseline) in mice bearing control tumors of MDA-MB-231 or MDA/pcDNA3. There was no significant difference between baseline and sacrifice values in mice bearing the MDA/TβRIIΔcyt tumors.

ment, the effect of factors known to be present in bone matrix were tested on PTHrP production by human MDA-MB-231 breast cancer cells *in vitro*. Only TGF-β significantly increased PTHrP production by these cells in a dose-dependent manner (Fig. 1*a*). Other growth factors abundant in bone, such as FGF-1 and -2, IGF-1 and -2, and PDGF, had no effect on PTHrP secretion over a wide range of concentrations.

Expression of a truncated type II TGF-β receptor (TβRIIΔ-cyt) in MDA-MB-231 cells. TGF-β was the only factor tested that affected PTHrP secretion, so its role in breast cancer metastasis to bone was investigated by transfecting MDA-MB-231 cells with the cDNA for a truncated type II TGF-β receptor (MDA/TβRIIΔcyt) and generating clonal lines. This receptor is truncated at the intracytoplasmic domain and has 199 amino acids and a predicted protein size of 22 kDa. A hemagglutinin (HA) epitope is present in the extracellular domain. The mutant receptor binds TGF-β, but because it cannot phosphorylate the type I receptor, signal propagation does not occur (23). Thus, it acts in a dominant-negative fashion to block the biologic effects of TGF-β.

As shown in Fig. 1*b*, treatment of parental MDA-MB-231 cells and the MDA/pcDNA3 clone with TGF-β1 (5 ng/ml) significantly stimulated PTHrP secretion, while the same treatment of three different MDA/TβRIIΔcyt resulted in minimal or no increase. Similar results were observed when the clones MDA/TβRIIΔcyt and MDA/pcDNA3 were grown in the absence of the selective marker, G418, for four weeks and indicate that TβRIIΔcyt was stably expressed. These data demonstrate that TβRIIΔcyt acts as a dominant-negative to block the biologic effects of TGF-β to stimulate PTHrP production by MDA-MB-231 breast cancer cells. In two separate pilot experiments using a mouse model of bone metastases, all three MDA/TβRIIΔcyt clones had smaller total osteolytic lesion area on radiographs compared with parental or empty vector controls (Fig. 1, *c* and *d*). Because MDA/TβRIIΔcyt clone 2 was the least responsive to TGF-β, it was studied in further detail.

Receptor expression in stable clones was demonstrated by cross-linking to ^{125}I-labeled TGF-β1. Figure 2*a* demonstrates the autoradiograph of ^{125}I-labeled TGF-β1 cross-linking followed by immunoprecipitation with anti-HA antibody in clonal MDA-MB-231 cells expressing the TβRIIΔcyt (MDA/TβRIIΔcyt, clone 2) or the empty vector (MDA/pcDNA3). Two distinct bands, which were completely competed by cold TGF-β, were present in MDA/TβRIIΔcyt. One band had a molecular weight corresponding to the predicted size of the truncated TGF-β type II receptor plus TGF-β dimer (47 kDa). The other band corresponded to the truncated type II TGF-β receptor plus TGF-β monomer, which has a predicted size of 34 kDa. No bands were evident by immunoprecipitation with the anti-HA antibody in the MDA/pcDNA3 clonal cells, which indicates that only MDA/TβRIIΔcyt expressed the truncated type II TGF-β receptor. These results also indicate that in the MDA/TβRIIΔcyt, this mutant TGF-β type II receptor was expressed at the cell surface and bound TGF-β. Endogenous type II TGF-β receptor was expressed by both cell lines, as demonstrated by ^{125}I-labeled TGF-β1 cross-linking followed by immunoprecipitation with a polyclonal type II TGF-β receptor antibody (data not shown).

Effect of TGF-β on growth of MDA-MB-231, MDA/pcDNA3, and MDA/TβRIIΔcyt clonal cells. Because TGF-β also regulates cellular functions of proliferation and differentiation, the effects of TGF-β on growth of parental MDA-MB-231, MDA/TβRIIΔcyt (clone 2) and MDA/pcDNA3 clonal cells were studied. As illustrated in Fig. 2*b*, growth rates were similar for all three cell lines in the absence of TGF-β. TGF-β1 (20 ng/ml) inhibited the growth of parental MDA-MB-231 and MDA/pcDNA3 cells but had

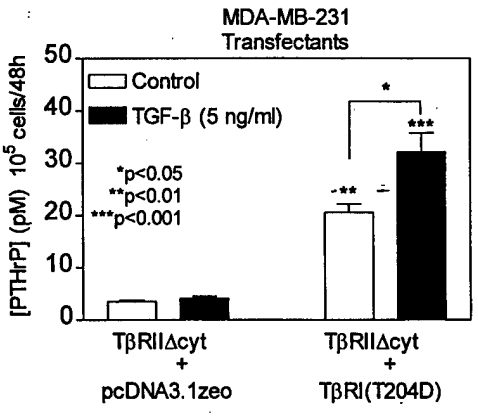

Figure 5
Effect of TGF-β on PTHrP secretion by MDA-MB-231 clonal lines, TβRIIΔ–cyt + TβRI(T204D), and TβRIIΔcyt + pcDNA3.1zeo. Respective cells were plated onto 48-well plates and treated as in Fig. 1*a*. Values represent the mean ± SEM (n = 3 per group). $^{**}P < 0.01$ and $^{***}P < 0.001$ compared with TβRIIΔcyt + pcDNA3.1zeo (control or TGF-β–stimulated).

Figure 6

(*a*) Representative radiographs of hindlimbs from mice bearing TβRIIΔ–cyt + TβRI(T204D) or TβRIIΔcyt + pcDNA3.1zeo 28 days after tumor inoculation. Osteolytic lesions are indicated by the arrows. (*b*) Osteolytic lesion number and area on radiographs as measured by computerized image analysis of forelimbs and hindlimbs. Respective tumor cells were inoculated on day 0. Values represent the mean ± SEM (n = 5 per group). (*c*) Histomorphometric analysis of hindlimbs from mice with osteolytic lesions. Data represent measurements from midsections of tibiae and femora of mice (from *b*) inoculated with either TβRIIΔcyt + TβRI(T204D) or TβRIIΔcyt + pcDNA3.1zeo tumors. Tumor area (mm^2) from metastatic bone lesions is illustrated on the right and osteoclast number per millimeter of tumor adjacent to bone (tumor/bone interface) on the left. Values represent the mean ± SEM. (*d*) Bone histology from the midtibial metaphysis of representative mice bearing either TβRIIΔcyt + TβRI(T204D) or TβRIIΔcyt + pcDNA3.1zeo tumors. Tumor (*arrows*) filled the marrow cavity and replaced normal cellular elements in mice bearing TβRIIΔcyt + TβRI(T204D) tumors (*right*). There was significant loss of both cortical and trabecular bone in this group, and tumor has eroded through the growth plate. In contrast, sections from mice bearing control TβRIIΔcyt + pcDNA3.1zeo tumors (*left*) had small foci of tumor in the marrow cavity (*arrows*) with little bone destruction, as evidenced by intact trabecular and cortical bone.

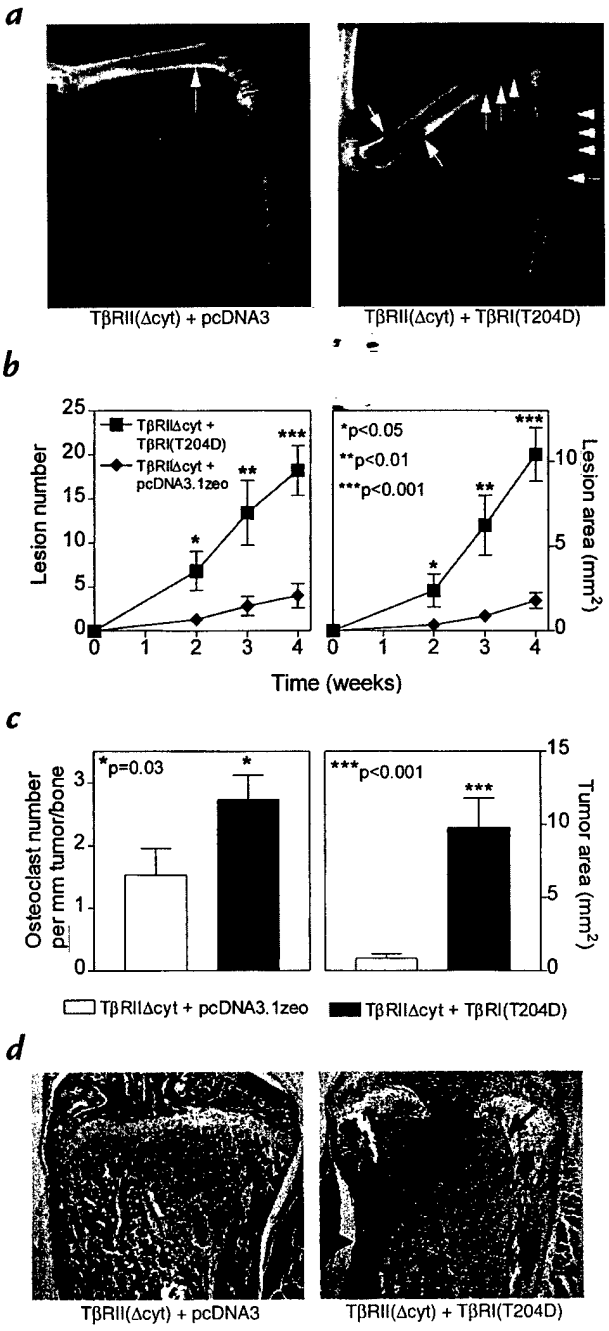

no effect on MDA/TβRIIΔcyt. Thus, expression of the dominant-negative receptor blocked TGF-β–mediated growth inhibition of MDA-MB-231 cells.

Role of TGF-β in breast cancer metastases to bone. To determine the effects of TGF-β on breast cancer–mediated osteolysis, MDA/TβRIIΔcyt (clone 2) or controls were studied in a mouse model of bone metastasis (17). Respective tumor cells were inoculated into the left cardiac ventricle of female nude mice, and serial radiographs were obtained. Representative radiographs from mice 24 days after tumor inoculation are illustrated in Fig. 3*a*. Osteolytic lesion number and area on radiographs were significantly less in MDA/TβRIIΔcyt-bearing mice compared with that of MDA/pcDNA3 and MDA-MB-231 controls (Fig. 3*b*). These data were consistent with the pilot experiments in which two other MDA/TβRIIΔcyt clones, in addition to clone 2, had significantly fewer and smaller bone metastases on radiographs compared with controls (Fig. 1, *c* and *d*).

Because radiographic methods assess only bone destruction and are not a direct measurement of tumor area in bone, histomorphometric analysis of forelimb and hindlimb bones was performed. Osteoclast number per millimeter of tumor/bone interface and tumor area in bone was significantly less in MDA/TβRIIΔcyt-bearing mice compared with MDA/pcDNA3 and MDA-MB-231 controls (Fig. 3*c*).

In a separate experiment, survival of mice bearing MDA/TβRIIΔcyt was significantly longer than that of the controls (Fig. 4*a*). In all experiments, there were no differences between MDA/TβRIIΔcyt and control groups with regard to metastasis to nonbone sites. Gross and histological assessment of soft tissues revealed little or no metastasis to adrenal glands, lungs, liver, spleen, ovaries, brain, or kidneys. In this survival experiment, plasma PTHrP concentrations were higher in the control groups, MDA/pcDNA3 and MDA-MB-231, at the time of death compared with baseline measurements. PTHrP concentrations did not differ from baseline to sacrifice in the MDA/TβRIIΔcyt group (Fig. 4*b*).

Effect of TβRIIΔcyt on local tumor growth. Although there were no differences in metastasis to nonbone sites between MDA/TβRIIΔcyt and control groups, there were insufficient metastases to determine whether expression of the dominant-negative receptor significantly affected tumor growth at sites other than bone. Thus, tumor-cell suspensions (10^7 cells/100 μl/mouse) of MDA/TβRIIΔcyt, MDA/pcDNA3, or MDA-MB-231 cells were inoculated intramuscularly into the right thigh of female athymic nude mice. Tumors were excised, measured, and weighed at sacrifice, 21 days after tumor inoculation.

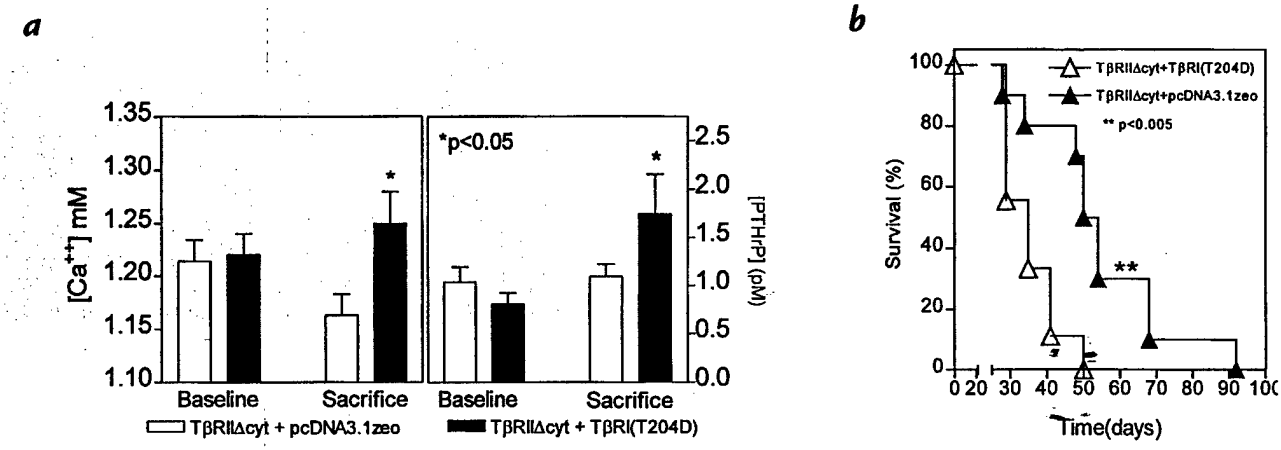

Figure 7

(*a*) Plasma PTHrP concentrations (*right*) and whole blood ionized calcium concentrations (*left*) at sacrifice were significantly higher than respective concentrations before tumor inoculation (baseline) in mice bearing tumors TβRIIΔcyt + TβRI(T204D). There was no significant difference between baseline and sacrifice values in mice bearing the control TβRIIΔcyt + pcDNA3.1zeo tumors. (*b*) Survival of mice bearing TβRIIΔcyt + TβRI(T204D) was significantly shorter than that of the controls, TβRIIΔcyt + pcDNA3.1zeo (n = 10 per group).

Tumor volume and tumor weight did not differ significantly between the groups (data not shown).

Restoration of TGF-β responsiveness into MDA/TβRIIΔcyt by expression of a constitutively active type I TGF-β receptor. To confirm that the decrease in bone metastasis was due to blockade of TGF-β signaling, the effects of the dominant-negative type II receptor mutation were reversed by the introduction of a constitutively active form of the type I receptor, TβR-I. This receptor has a point mutation at amino acid 204 of the GS domain in which aspartic acid replaces threonine (T204D). In TGF-β signal transduction, TβR-II phosphorylates TβR-I, which then propagates the signal (28). TβRI(T204D) is constitutively phosphorylated and does not require ligand binding or interaction with the type II receptor to mediate TGF-β signaling (24). TGF-β did not stimulate PTHrP production in the TβRIIΔcyt + pcDNA3.1zeo clone (empty vector control). However, there was a fivefold increase in the basal production of PTHrP by the TβRIIΔcyt + TβRI(T204D) clone that was further enhanced by TGF-β (Fig. 5). Thus, expression of the constitutively active TGF-β type I receptor overcame the dominant-negative blockade and restored the TGF-β-stimulated PTHrP production.

Next, to study the effect of the restoration of TGF-β responsiveness, MDA-MB-231 clonal lines of TβRIIΔcyt + TβRI(T204D) or TβRIIΔcyt + pcDNA3.1zeo control cells were inoculated into the left cardiac ventricle of female nude mice, and serial radiographs were obtained. Four weeks after tumor inoculation, mice bearing TβRIIΔcyt + TβRI(T204D) tumors had significantly more and larger osteolytic lesions on radiographs compared with those bearing TβRIIΔcyt + pcDNA3.1zeo tumors (Fig. 6, *a* and *b*). Histomorphometric analysis of hindlimbs supported the radiographic findings and revealed that the osteoclast number per millimeter of tumor/bone interface and tumor area in bone was significantly greater in the TβRIIΔcyt + TβRI(T204D) group when compared with the control group, TβRIIΔcyt + pcDNA3.1zeo (Fig. 6*c*). Histological sections of the midtibial metaphysis from mice bearing TβRIIΔcyt + TβRI(T204D) demonstrate tumor replacing the marrow cavity and destruction of both trabecular and cortical bone, whereas bones from mice bearing TβRIIΔcyt + pcDNA3.1zeo had small foci of tumor in the bone marrow cavity with little bone destruction (Fig. 6*d*). Plasma PTHrP and blood ionized calcium concentrations were also significantly higher in mice bearing TβRIIΔcyt + TβRI(T204D) tumors compared with those bearing the control, TβRIIΔcyt + pcDNA3.1zeo (Fig. 7*a*). In a separate experiment, mice bearing the TGF-β-responsive tumor, TβRIIΔcyt + TβRI(T204D), had a significantly shorter survival time than mice bearing the tumors that were unresponsive to TGF-β (Fig. 7*b*).

Overexpression of PTHrP, under the control of a constitutive promoter, into MDA/TβRIIΔcyt. To determine whether the effects of TGF-β to enhance bone metastases were mediated by PTHrP, the MDA/TβRIIΔcyt clonal line was transfected with the cDNA encoding human pre-proPTHrP-(1-141) under the control of a constitutive CMV promoter. Figure 8*a* demonstrates that basal PTHrP secretion *in vitro* was greater in two different TβRIIΔcyt + PTHrP clones compared with the TβRIIΔcyt + pcDNA3.1zeo control. PTHrP secretion did not increase in response to TGF-β in any clone expressing the dominant-negative type II receptor (Fig. 8*a*). Next, the effect of PTHrP overexpression by MDA/TβRIIΔcyt was studied *in vivo*. Thirty-one days after tumor inoculation, mice bearing either TβRIIΔcyt + PTHrP clone had significantly larger and more osteolytic lesions on radiographs compared with those bearing TβRIIΔcyt + pcDNA3.1zeo tumors (Fig. 8, *b* and *c*). At the time of sacrifice, plasma PTHrP concentrations (Fig. 8*d*) were significantly greater in both TβRIIΔcyt + PTHrP groups compared with the TβRII-cyt + pcDNA3.1zeo control group, as were blood ionized calcium concentrations (data not shown).

Discussion

Breast cancer metastasizes to bone in greater than 80% of patients with advanced disease and causes local bone destruction (2) with subsequent pain, fracture, hyper-

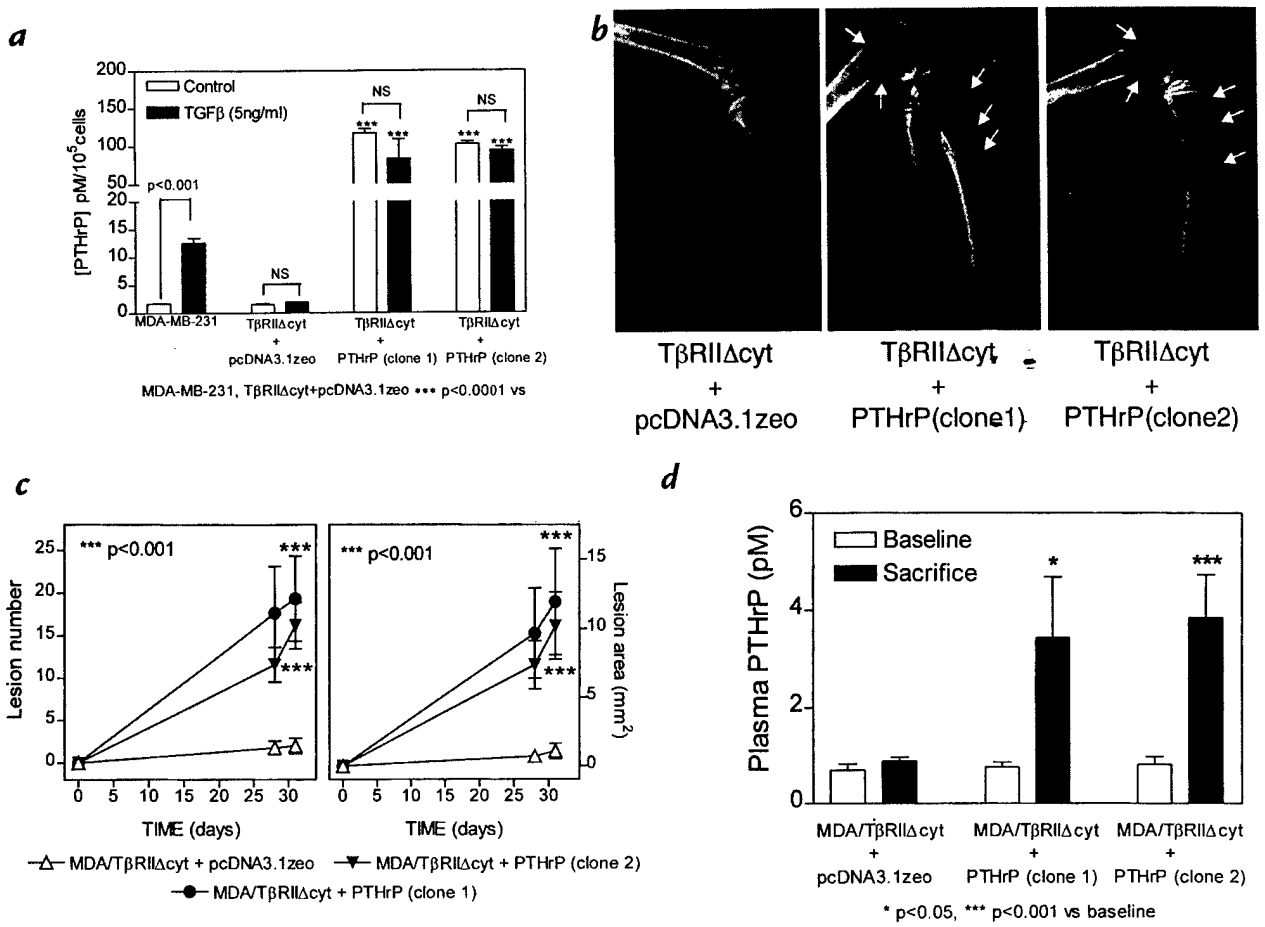

Figure 8

(*a*) Effect of TGF-β on PTHrP secretion by MDA-MB-231 and MDA/TβRIIΔcyt cell clones that overexpress PTHrP (*TβRIIΔcyt + PTHrP*; two clones) or the empty vector (*TβRIIΔcyt + pcDNA3.1zeo*). Respective cells were plated onto 48-well plates and treated as in Fig. 1*a*. Values represent the mean ± SEM (n = 3 per group). (*b*) Representative radiographs of hindlimbs from mice bearing two different TβRIIΔcyt + PTHrP clones or TβRIIΔcyt + pcDNA3.1zeo control 31 days after tumor inoculation. Osteolytic lesions are indicated by the arrows. (*c*) Osteolytic lesion number and area on radiographs as measured by computerized image analysis of forelimbs and hindlimbs. Respective tumor cells were inoculated on day 0. Values represent the mean ± SEM (n = 5) per group. (*d*) Plasma PTHrP concentrations at sacrifice were significantly higher than respective concentrations prior to tumor inoculation (baseline) in mice bearing either TβRIIΔcyt + PTHrP tumors. There was no significant difference between baseline and sacrifice values in mice bearing the control TβRIIΔcyt + pcDNA3.1zeo tumors.

calcemia, and nerve compression syndromes. The data presented here suggest a central role for TGF-β in the pathogenesis of breast cancer metastasis to bone. Breast cancer cells that metastasizes to bone stimulate osteoclastic bone resorption (5–7, 29) and release of active TGF-β into the bone microenvironment (4). This increase in locally active TGF-β alters tumor-cell behavior to promote growth and bone destruction at the metastatic site. Thus, in the situation of breast cancer metastases to bone, it appears that host-derived TGF-β acts on the tumor cells, via a receptor-mediated mechanism, to endow metastatic capacity rather than a case of tumor-derived TGF-β acting on the mesenchyme to favor invasion. In the results reported here, TGF-β has the paradoxical effect of enhancing metastasis and bone destruction while inhibiting tumor-cell growth *in vitro*.

Dominant-negative blockade of the type II TGF-β receptor had no effect on cell growth *in vitro* in the absence of TGF-β or on cell growth of tumor cells inoculated intramuscularly, but it significantly decreased tumor growth in bone. In contrast, expression of the dominant-negative type II TGF-β receptor blocked the growth inhibitory effects of TGF-β *in vitro*. On the basis of the growth results *in vitro*, one might expect the MDA/TβRIIΔcyt cells to grow more rapidly in bone, when, in fact, these cells had a much slower growth rate in bone compared with the controls.

It has been suggested that breast cancer cells may progress from a growth-inhibited to a growth-stimulated response to TGF-β (30). Previous work in breast cancer has focused on the growth inhibitory effects of TGF-β, as exemplified by the findings that TGF-β1 suppresses mammary tumorigenesis in mouse mammary tumor virus/TGF-β1 transgenic mice (31). Furthermore, expression of a type II TGF-β receptor in the human breast cancer cell line, MCF-7, diminished tumorigenicity (32), whereas transgenic mice overexpressing a dominant-negative mutant type II TGF-β receptor had enhanced tumorigenesis in the mammary gland and lung in response to the carcinogen 7,12-dimethylbenz-[*a*]-

anthracene (33). The data presented here, however, suggest that the effects of TGF-β unrelated to growth inhibition in the context of tumor-host interaction can negatively affect the host. This paradigm goes against the simple idea that losing responsiveness to TGF-β is universally permissive for transformation. In fact, the results suggest that maintenance of TGF-β receptors on the tumor cells can adversely affect the host by an indirect effect on the metastatic process.

Although loss of TGF-β receptor function (34) or its signaling molecules (35–38) has been associated with malignant progression (28), there is growing evidence that TGF-β may enhance tumor growth and invasion. In a transgenic mouse model in which TGF-β1 expression was targeted to keratinocytes, TGF-β1 had a biphasic action during skin carcinogenesis by acting early as a tumor suppressor and later by enhancing a malignant phenotype (39). TGF-β has also been shown to induce an epithelial-mesenchymal transdifferentiation to an invasive phenotype (40, 41). Mammary epithelial cells transformed by Ras can become resistant to growth inhibition by TGF-β (42). Furthermore, in these cells, TGF-β enhances invasion and tumorigenesis by inducing a highly motile fibroblastoid phenotype. A possible basis for this is the ability of Ras-activated Erk to phosphorylate and inhibit Smad proteins (43). An oncogenic Ras mutation has been reported in MDA-MB-231 breast cancer cells (44). This may explain why these cells are only moderately growth-inhibited by TGF-β *in vitro*, as well as why cells expressing the constitutively active type I TGF-β receptor develop severe bone metastases, a phenotype that indicates excessive tumor growth in bone.

The effects of TGF-β in cancer may be tissue-specific. In recent work by Böttinger *et al.* (45), targeted expression of a dominant-negative type II TGF-β receptor in pancreas and liver resulted in pancreatic carcinoma without liver abnormalities. The results presented here are also consistent with a tissue-specific role of TGF-β in malignancy. In the situation of breast cancer metastasis to bone, TGF-β, released and activated as a result of tumor-stimulated osteoclastic bone resorption, is an important segment of a paracrine loop that may be responsible for the affinity with which breast cancer grows in bone. In tumor cells with oncogenic Ras mutations, TGF-β may promote further tumor development. The data presented here also suggest the possibility that PTHrP may be an effector of TGF-β in bone metastases, because overexpression of PTHrP into the breast cancer cells that expressed the dominant-negative TGF-β type II receptor resulted in accelerated bone metastases. The effect of TGF-β on tumor cells to stimulate PTHrP may result in adverse effects only when tumor cells are housed in bone rather than in soft tissue sites. Tumor cells in the bone microenvironment produce PTHrP and stimulate osteoclastic bone resorption, which in turn results in the release of active TGF-β. TGF-β then acts on the tumor cells to endow them with metastatic capacity and the ability to stimulate production of PTHrP. The net result is tumor growth, bone destruction, fracture, and the complications of osteolytic bone metastases.

Acknowledgments

The authors thank Yong Cui and Suzanne D. Taylor for technical assistance, and Kohei Miyazano for antiserum against the human TGF-β type II receptor. This work was supported by National Institutes of Health grants AR01899 and CA69158 (to T.A. Guise), CA40035 and AR28149 (to G.R. Mundy), a National Cancer Institute Breast Cancer Spore grant (to J. Massagué), and a San Antonio Cancer Institute grant (to T.A. Guise). J.M. Chirgwin is a Veterans Administration Associate Research Career Scientist. J. Massagué is a Howard Hughes Medical Investigator.

1. Paget, S. 1889. The distribution of secondary growths in cancer of the breast. *Lancet.* 1:571–572.
2. Coleman, R.E., and Rubens, R.D. 1987. The clinical course of bone metastases from breast cancer. *Br. J. Cancer.* **55**:61–66.
3. Hauschka, P.V., Mavrakos, A.E., Iafrati, M.D., Doleman, S.E., and Klagsbrun, M. 1986. Growth factors in bone matrix. *J. Biol. Chem.* **261**:12665–12674.
4. Pfeilschifter, J., and Mundy, G.R. 1987. Modulation of transforming growth factor β activity in bone cultures by osteotrophic hormones. *Proc. Natl. Acad. Sci. USA.* **84**:2024–2028.
5. Boyde, A., Maconnachie, E., Reid, S.A., Delling, G., and Mundy, G.R. 1986. Scanning electron microscopy in bone pathology: review of methods. Potential and applications. *Scanning Electron Microsc.* **4**:1537–1554.
6. Hortobagyi, G.N., *et al.* 1996. Efficacy of pamidronate in reducing skeletal complications in patients with breast cancer and lytic bone metastases. *N. Engl. J. Med.* **335**:1785–1791.
7. Diel, I.J., *et al.* 1998. Reduction in new metastases in breast cancer with adjuvant clodronate treatment. *N. Engl. J. Med.* **339**:357–363.
8. Burtis, W.J., *et al.* 1987. Identification of a novel 17,000-dalton parathyroid hormone-like adenylate cyclase-stimulating protein from a tumor associated with humoral hypercalcemia of malignancy. *J. Biol. Chem.* **262**:7151–7156.
9. Moseley, J.M., *et al.* 1987. Parathyroid hormone-related protein purified from a human lung cancer cell line. *Proc. Natl. Acad. Sci. USA.* **84**:5048–5052.
10. Strewler, G.J., *et al.* 1987. Parathyroid hormone-like protein from human renal carcinoma cells structural and functional homology with parathyroid hormone. *J. Clin. Invest.* **80**:1803–1807.
11. Jüppner, H., *et al.* 1991. A G protein-linked receptor for parathyroid hormone and parathyroid hormone-related peptide. *Science.* **254**:1024–1026.
12. Abou-Samra, A., *et al.* 1992. Expression cloning of a common receptor for parathyroid hormone and parathyroid hormone-related peptide from rat osteoblast-like cells: a single receptor stimulates intracellular accumulation of both cAMP and inositol triphosphates and increases intracellular free calcium. *Proc. Natl. Acad. Sci. USA.* **89**:2732–2736.
13. Burtis, W.J., *et al.* 1990. Immunochemical characterization of circulating parathyroid hormone-related protein in patients with humoral hypercalcemia of cancer. *N. Engl. J. Med.* **322**:1106–1112.
14. Bundred, N.J., *et al.* 1991. Parathyroid hormone related protein and hypercalcaemia in breast cancer. *Br. Med. J.* **303**:1506–1509.
15. Powell, G.J., *et al.* 1991. Localization of parathyroid hormone-related protein in breast cancer metastasis: increased incidence in bone compared with other sites. *Cancer Res.* **51**:3059–3061.
16. Southby, J., *et al.* 1990. Immunohistochemical localization of parathyroid hormone-related protein in breast cancer. *Cancer Res.* **50**:7710–7716.
17. Guise, T.A., *et al.* 1996. Evidence for a causal role of parathyroid hormone-related protein in breast cancer-mediated osteolysis. *J. Clin. Invest.* **98**:1544–1548.
18. Zakalik, D., Diep, D., Hooks, M.A., Nissenson, R.A., and Strewler, G.J. 1992. Transforming growth factor β increases stability of parathyroid hormone-related protein messenger RNA. *J. Bone Miner. Res.* **7**:104A, S118.
19. Kiriyama, T., *et al.* 1992. Transforming growth factor β stimulation of parathyroid hormone-related protein (PTHrP): a paracrine regulator? *Mol. Cell. Endocrinol.* **92**:55–62.
20. Merryman, J.I., DeWille, J.W., Werkmeister, J.R., Capen, C.C., and Rosol, T.J. 1994. Effects of transforming growth factor-β on parathyroid hormone-related protein production and ribonucleic acid expression by a squamous carcinoma cell line *in vitro*. *Endocrinology.* **134**:2424–2430.
21. Southby, J., Murphy, L.M., Martin, T.J., and Gillespie, M.T. 1996. Cell-specific and regulator-induced promoter usage and messenger ribonucleic acid splicing for parathyroid hormone-related protein. *Endocrinology.* **137**:1349–1357.
22. Cailleau, R., Yong, R., Olive, M., and Reeves, W.J. 1974. Breast tumor cell lines from pleural effusions. *J. Natl. Cancer Inst.* **53**:661–674.
23. Wieser, R., Attisano, L., Wrana, J.L., and J. Massagué. 1993. Signaling activity of transforming growth factor β type II receptors lacking specific domains in the cytoplasmic region. *Mol. Cell. Biol.* **13**:7239–7247.
24. Wieser, R., Wrana, J.L., and Massagué, J. 1995. GS domain mutations that constitutively activate T beta R-I, the downstream signaling com-

ponent in the TGF-beta receptor complex. *EMBO J.* **14**:2199–2208.
25. Cárcamo, J., *et al.* 1994. Type I receptors specify growth-inhibitory and transcriptional responses to transforming growth factor β and activin. *Mol. Cell. Biol.* **14**:3810–3821.
26. Guise, T.A., Chirgwin, J.M., Favarato, G., Boyce, B.F., and Mundy, G.R. 1992. Chinese hamster ovarian cells transfected with human parathyroid hormone-related protein cDNA cause hypercalcemia in nude mice. *Lab. Invest.* **67**:477–485.
27. Pandian, M.R., Morgan, C.H., Carlton, E., and Segre, G.V. 1992. Modified immunoradiometric assay of parathyroid hormone-related protein: clinical application in the differential diagnosis of hypercalcemia. *Clin. Chem.* **38**:282–288.
28. Massagué, J. 1998. TGF-β signal transduction. *Annu. Rev. Biochem.* **67**:753–791.
29. Sasaki, A., *et al.* 1995. The bisphosphonate risedronate reduces metastatic human breast cancer burden in bone in nude mice. *Cancer Res.* **55**:3551–3557.
30. Arteaga, C.L., Dugger, T.C., and Hurd, S.D. 1996. The multifunctional role of transforming growth factor (TGF)-βs on mammary epithelial cell biology. *Breast Cancer Res. Treat.* **38**:49–56.
31. Pierce, D.F., Jr., *et al.* 1995. Mammary tumor suppression by transforming growth factor β1 transgene expression. *Proc. Natl. Acad. Sci. USA.* **92**:4254–4258.
32. Sun, L., *et al.* 1994. Expression of transforming growth factor β type II receptor leads to reduced malignancy in human breast cancer MCF-7 cells. *J. Biol. Chem.* **269**:26449–26455.
33. Böttinger, E.P., Jakubczak, J.L., Haines, D.C., Bagnall, K., and Wakefield, L.M. 1997. Transgenic mice overexpressing a dominant-negative mutant type II transforming growth factor β receptor show enhanced tumorigenesis in the mammary gland and lung in response to the carcinogen 7,12-dimethylbenz-[*a*]-anthracene. *Cancer Res.* **57**:5564–5569.
34. Markowitz, S., *et al.* 1995. Inactivation of the type II TGF-β receptor in colon cancer cells with microsatellite instability. *Science.* **268**:1336–1338.
35. Eppert, K., *et al.* 1996. MADR2 maps to 18q12 and encodes a TGFβ-regulated MAD-related protein that is functionally mutated in colorectal carcinoma. *Cell.* **88**:543–552.
36. Zhu, Y., Richardson, J.A., Parada, L.F., and Graff, J.M. 1998. Smad3 mutant mice develop metastatic colorectal cancer. *Cell.* **94**:703–714.
37. Hahn, S.A., *et al.* 1996. DPC4, a candidate tumor suppressor gene at human chromosome 18q21.1. *Science.* **271**:259–253.
38. Takaku, K., *et al.* 1998. Intestinal tumorigenesis in compound mutant mice of both Dpc4 (Smad4) and Apc genes. *Cell.* **92**:645–656.
39. Cui, W.E., *et al.* 1996. TGFβ1 inhibits the formation of benign skin tumors, but enhances progression to invasive spindle carcinomas in transgenic mice. *Cell.* **86**:531–542.
40. Caulin, C., Scholl, S.G., Frontelo, P., Gamallo, C., and Quintanilla, M. 1995. Chronic exposure of cultured transfected mouse epidermal cells to TGFβ1 induces an epithelial-mesenchymal transdifferentiation and a spindle tumoral phenotype. *Cell Growth Differ.* **6**:1027–1035.
41. Miettinen, P.J., Ebner, R., Lopez, A.R., and Derynck, R. 1994. TGF-β induced transdifferentiation of mammary epithelial cells to mesenchymal cells: involvement of type I receptors. *J. Cell Biol.* **127**:2021–2036.
42. Oft, M., *et al.* 1996. TGF-β1 and Ha-Ras collaborate in modulating the phenotypic plasticity and invasiveness of epithelial tumor cells. *Genes Dev.* **10**:2462–2477.
43. Kretzschmar, M., Doody, J., and Massagué, J. 1997. Opposing BMP and EGF signalling pathways converge on the TGF-β family mediator Smad1. *Nature.* **389**:618–622.
44. Sepp-Lorenzino, L., *et al.* 1995. A peptidomimetic inhibitor of farnesyl:protein transferase blocks the anchorage-dependent and -independent growth of human tumor cell lines. *Cancer Res.* **55**:5302–5309.
45. Böttinger, E.P., *et al.* 1997. Expression of a dominant-negative mutant TGF-β type II receptor in transgenic mice reveals essential roles for TGF-β in regulation of growth and differentiation in the exocrine pancreas. *EMBO J.* **16**:2621–2633.